INTEGRATING GIS AND HYDROLOGY

FOR FLOOD RISK ANALYSIS

Anas B. Rabie

58 Pages August 2014

Spatial analysis using GIS was evaluated for its ability to predict the potential hazard of a flood event in the Illinois River region in the State of Illinois. The data employed in the analysis are available to the public from trusted organizations such as Illinois State Geological Survey (ISGS), and the US Geological Survey (USGS). The purposes of this study are to 1) examine the applicability of GIS spatial analysis to determine flood inundation risk, and 2) to determine how to do so with the least amount of data possible, while still producing an accurate flood inundation risk map. This study concentrates on areas that have stream gauge data with definable flood stage(s) and utilizes the Inverse Distance Weighted (IDW) spatial analysis interpolation method on different digital elevation models (DEM) with different resolutions to determine the potential flood level over the study area. Resulting maps created for the Illinois River region yielded about 80% agreement to the actual effects of the Illinois River flood near Peoria on April 23rd, 2013. As a result, it was concluded that it is possible to create a decent flood prediction map using only two initial input data layers: stream gauges, and a digital elevation model (DEM).

INTEGRATING GIS AND HYDROLOGY

FOR FLOOD RISK ANALYSIS

ANAS B. RABIE

A Thesis Submitted in Partial
Fulfillment of the Requirements
for the Degree of

MASTER OF SCIENCE

Department of Geography-Geology

ILLINOIS STATE UNIVERSITY

2014

INTEGRATING GIS AND HYDROLOGY

FOR FLOOD RISK ANALYSIS

ANAS B. RABIE

COMMITTEE MEMBERS:

Eric W. Peterson, Chair

John Kostelnick, Co-Chair

Rex J. Rowley

ACKNOWLEDGMENTS

Grateful thanks goes to the members of my committee; Dr. Eric Peterson, Dr. John Kostelnick, and Dr. Rex J. Rowley, for their close supervision and advice. My appreciation is due to Dr. Lisa Tranel for her guidance and supervision during the early stages of the work. In addition, a special thanks to Dr. Jonathan B. Thayn for his help and advice during different processes in the project. Finally, the author wish to the thank all who helped during the course of this report.

A.B.R.

CONTENTS

TABLES

FIGURES

CHAPTER I

INTRODUCTION

Flood Risk and Uncertainty

Rainfall and runoff gauges are not readily available for every river system, which affects the credibility and availability of hydrological data. In addition, due to the vigorous urbanization activities in some areas, as well as temporal and spatial variation of hydrological characteristics, the quantitative assessment of runoff characteristics in most areas is not straightforward (El Hames et al, 1998). Sometimes much of the uncertainty associated with flood events is linked to a lack of accurate environmental data (Barroca, 2006). This absence of data may be because of civilian tampering with gauges and measurement devices, or, more likely, a lack of continuous maintenance and monitoring. Knowing what causes a flood and a flood's impacts is important, however, in order to avoid any tragedy in the future, especially in the context of climate change and intensive urbanization (El-Hames et al, 2012).

Natural variability and uncertainty create ambiguity in the floodplain boundary. Natural variability is the inherent changing of the floodplain boundary because of natural processes. Examples of hydrologic and hydraulic characteristics having natural variability include predicted (historically or mathematically) stream flows, precipitation, soil

properties, and floodplain roughness. Uncertainty refers to incomplete information about the process leading to flooding in a floodplain, which leads to ambiguity in measuring the flood characteristics (Smemoe et al, 2007).

Many factors can affect flood characteristics. These factors include precipitation, ambient soil water content, land use, evaporation intensity, watershed infiltration, and geology and geomorphology of the area. Each of these factors also impacts the other significantly, and their complex relationship affects the runoff. In order to be able to create an accurate hydrological model, a good grasp of the interaction between these factors is mandatory (Kia et al, 2012). However, we are limited by the data we can use to model a flood. The critical data needed to do so are land elevation and water level. As noted above, these data may not always be available, may not be ready to use, or the quality of the data may vary significantly.

Importance of Flood Risk Maps

Basic maps depicting floodwater distribution that provide continuous and rapid simulations – which can be considered "an effective real-time flood modeling and prediction system" (Al-Sabhan et al., 2003, p.10) – could give decision makers an understanding of the threatened areas. Such understanding will eventually help avoid future flood disasters The Federal Emergency Management Agency (FEMA) in the United States usually creates their maps using a combination of eight different factors: aerial imagery, elevation, geodetic control, boundaries, surface waters, transportation, land ownership, and special flood hazard areas (Lowe, 2003). Some studies that

attempted to understand flood risks using spatial analysis agree on one assumption: peak floods are "stationary with time" (Cameron et al., 1999; Wigley et al., 1992; Arnell et al., 1996). Paradoxically, while some studies suggest that this is only true if the physical and hydrological characteristics of the catchment can be considered constant in the long-term, other studies demonstrated the variability of climate characteristics as the potential cause for more intense hydrological impacts as a result of future climate change (e.g. Hulme et al, 1999; Wigley et al., 1992; Pilling et al., 1998). It is important to point out that climate change may have serious implications for flood frequency (Panagoulia et al., 1997; Naden et al., 1996). Still, the development of new numerical methods helps improve the predictability of the consequences of flood events (Beffa, 1998; Connell et al., 1998). As Beffa (2000, 1) explained, with the use of high quality terrain data, such as Digital Elevation Models (DEM) or Light Detection and Ranging (LiDAR) DEM data, "it is possible to make flood predictions that are relevant, meaningful, and logically correct."

Overview Background

Geographic Information Systems (GIS) is used for the storage, management, analysis and mapping of spatial data. Integration of GIS technologies with other data has resulted in an intelligent form of data analysis that can make use of the spatial patterns within the data in order to plot the data on maps for easy operation and interpretation (Farmahan, 2012). While many watershed modeling software packages are currently available, few are well integrated within spatial modeling environments and are capable of non-expert application (Al-Sabhan et al., 2003). Furthermore, considering the fact that LiDAR DEM datasets have higher spatial resolution than standard DEM datasets (30m

and 10m standard for non-LiDAR DEMs and 3m and 1m for LiDAR DEMs), a comparison between the different resolutions is necessary to enrich the understandings of any value added given the high expense in acquiring LiDAR datasets. Figure 1 shows a basic comparison between a low resolution DEM and a high resolution DEM. The availability of adequate data for the study areas from well-known sources makes it easier to generate a prediction map filled with data, where it is then possible to start reducing the amount of data until the point of the minimum requirements to generate results at an acceptable accuracy level.

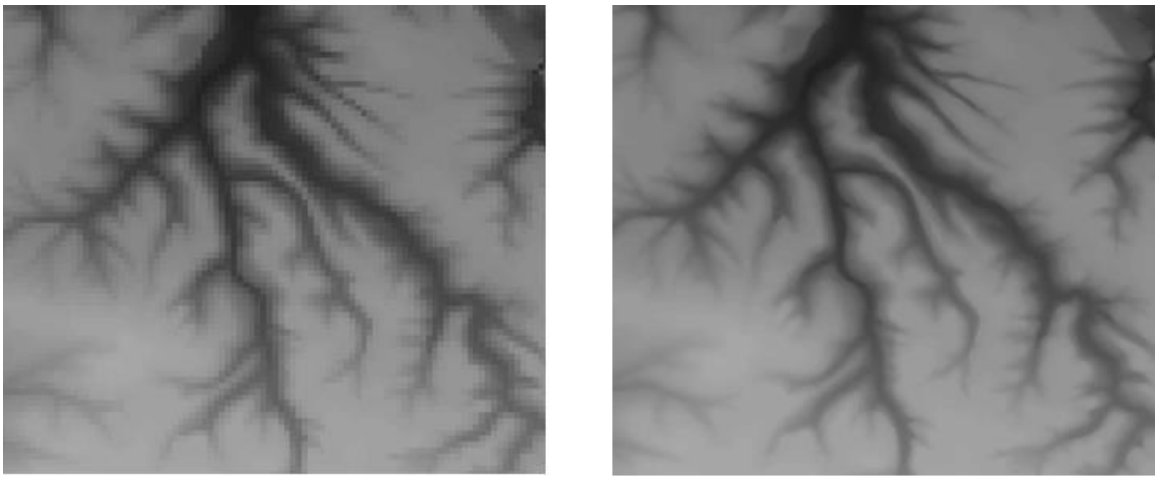

Figure 1: The difference in clarity of the low-resolution (30m) DEMs vs higher-resolution DEM (10m).

The Different Approaches

The fact that the term "flood risk" usually indicates natural disasters implies several definitions. The level of risk depends on the natural disaster's significance on

human lives, and/or the economy (Safaripour et al., 2012). Furthermore, flood risk can be looked upon to identify either vulnerability (the risk of a flood) or hazard (the actual flood occurrence). This distinction has opened the way for scholars and researchers to study flood risk from various perspectives. Determining flood risk by investigating the historic frequency of floods is a common method used by previous studies. Lawrence (1999) studied 30 major characteristics of floods to find out which influence the ecological risk. Yalcin (2004) used ArcGIS software to create a multi-phase evaluation process to indicate vulnerability to flood. Similarly, Sinnakudan (2003) explained the validity of using the AVHEC-6 extension of the ArcView software in modeling a flood map. Furthermore, Hansson (2008) presented a strategic assessment of flood damage using computerized multi-phase analysis methods.

Study Purpose and Hypothesis

The present study provides a demonstration of the viability of creating a flood risk map using stream gauges density and DEM spatial resolution as the two significant factors in determining vulnerability and hazard in GIS environment. In other words, the goal of this research is to investigate the applicability and effectiveness of GIS methods along with the role of digital terrain and stream gauge data to produce accurate simulations of a real-life flood event. Additionally, this study evaluates the minimum amount of data required to produce an accurate GIS model by comparing flood model results from various DEM resolutions coupled with varying combinations of stream gauges. The effectiveness of the model is tested by comparing the predictions to an actual flood extent through an accuracy assessment of each flood prediction.

The approach taken in this study is meant to show how to develop a model that is practical and can be applied to a wide variety of scenarios where flood hazards data input can be relayed to any system regardless of the amount of data available. This study is concerned with the model used, as well as the provision of a methodology for a rapid, easy-to-use, and cost-effective means for implementing flood hazard models.

I hypothesize that it is possible to produce a spatial model that addresses the issue of finding a simplified way to predict floods. Such simplified spatial models would be of great assistance to decision makers and city planners for forecasting a flood event in the selected environment, without a large input data requirement. Furthermore, a simplified model is easier to implement by personnel, especially those who are not flood engineers. It will also be helpful for decision makers to make the best choices for future development planning of a vulnerable area. A DEM, which is readily available for all of the United States at a relatively high resolution and for most of the world at a moderate resolution, is the most important factor in the models I will be testing.

Another hypothesis is that the generation of flood risk index maps using highly detailed data provided by trusted sources gives the results strength and better meaning. A key supposition in this hypothesis is that the higher resolution LiDAR DEMs will require fewer stream gauges to produce an accurate model that can simulate a flood event compared to the stream gauge density needed for a similarly accurate model created from the lower-resolution DEMs.

Furthermore, it is hypothesized that the higher the stream gauge density (e.g., number of stream gauges used), the more accurate flood model will result. Correspondingly, this rationale is hypothesized to be true regardless of the spatial analysis methods used to generate the flood model (e.g., Inverse Distance Weighting, Kriging). To evaluate the resulting flood risk maps, these maps were compared against an actual flood event map generated from satellite data collected near the peak of that event. After that, areas of agreement, over estimate and under estimate were calculated. Figure 2 shows the expected outcome of the simulations.

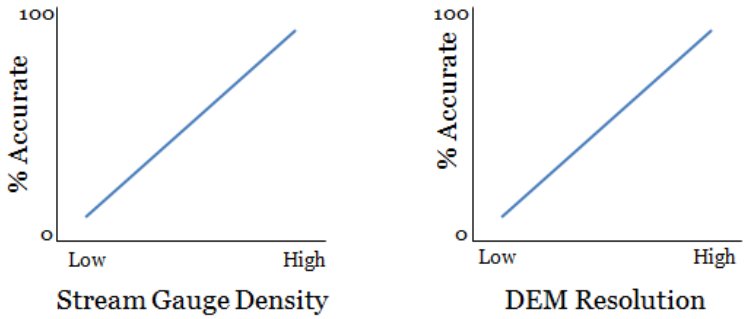

Figure 2: Charts showing the hypothesized results for the current study

CHAPTER II

METHODS

Study Area

The study was conducted on a portion of the Illinois River basin in the State of Illinois. This area was chosen because of the availability of all the needed data. These data includes digital elevation models (DEMs) at different spatial resolutions, working stream gauges with predefined flood levels, as well as satellite data for a recent flood event that affected the area in spring 2013, which is the source for the accuracy assessment for the predicted flood models.

The portion of the Illinois River basin in the State of Illinois (Figure 3) used in this study has a length of almost 225 km and drainage of roughly 36,350 km^2. The Illinois River is a major tributary of the Mississippi River. The Illinois River drainage basin counts for 44% of the State of Illinois land area. In addition, it links Lake Michigan in the northeast of the state to the Mississippi River (Lian, et al., 2012). Humans have modified the Illinois River watershed heavily by agriculture and other means (Sing, 1996). In order to keep a suitable water depth for ships movement, seven locks and dams were built on the Illinois River. The lower Illinois River floodplain is used for agriculture, thus levee

and drainage constructions are present (Lian, et al., 2012), this fact may have an impact on floodplain flooding, and potentially on the resulting analysis.

Geographically, the study area at the Illinois River extends from Cass and Schuyler Counties in the south to La Salle County in the north. At the southern end of the region, an alluvial belt dominates the bottomlands with a width ranging from about five to six kilometers. This belt covers the southern banks of the Illinois River (Worthen, et al., 1868). The southernmost parts are prairies that have thin wood belts skirting the channel. To the north of that are broken hilly bluffs that run parallel to the streams. Six stream gauges are available along the river within the study area: at La Salle in La Salle County, at Henry in Marshall County, two stream gauges east and south-east of Peoria in Peoria County, at Havana in Mason County, and at Beardstown in Cass County.

The river follows a west course at the northern part of the study area. At the northernmost point of study area's extent, the Illinois River meets its principal tributaries: the Fox River and Big and Little Vermilion Rivers. Galena limestone and St. Peters sandstone are the two dominant geological formations at this end of the studied area.

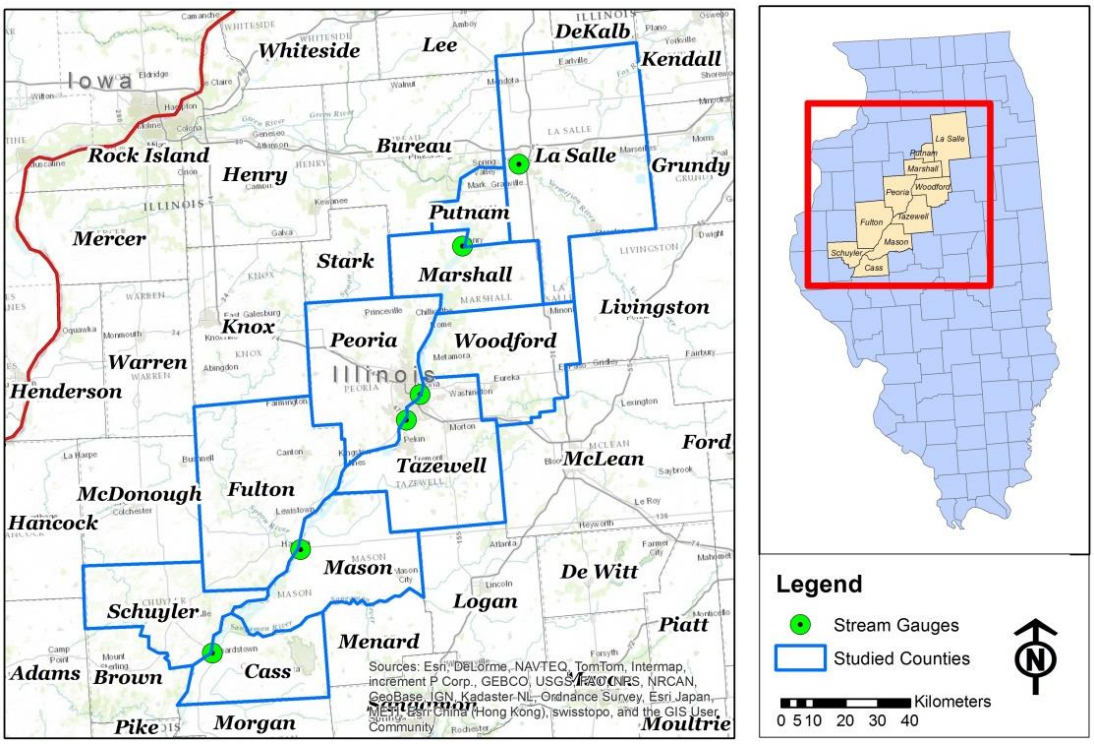

Figure 3: Map of the Illinois River Study Area.

GIS Data Use

Data were collected from different online and free data sources that provided hydrographical, elevation, topographical, and related data for the study area. DEMs for the study area were acquired from the USGS National Map Viewer with different resolutions – 30m, 10m, and 1m. Hydrography data include polygon water bodies and flow paths as lines from the National Hydrography Dataset (NHD). Stream gauges, including pre-defined flood stage levels data for the Illinois River system, were available from the National Weather Services (NWS) website. General layers for the states and counties were obtained from a compact disc (CD) that was provided with an ArcGIS tutorial book (Price, 2012). For accuracy assessment purposes, Landsat 8 Operational

Land Imager (OLI) imagery was acquired from the USGS Global Visualization Viewer (GLOVIS). All data were then incorporated into ArcGIS v.10.2 (ESRI 2013). Figure 4 illustrates the GIS methodology used to derive the flood predictions and accuracy assessment.

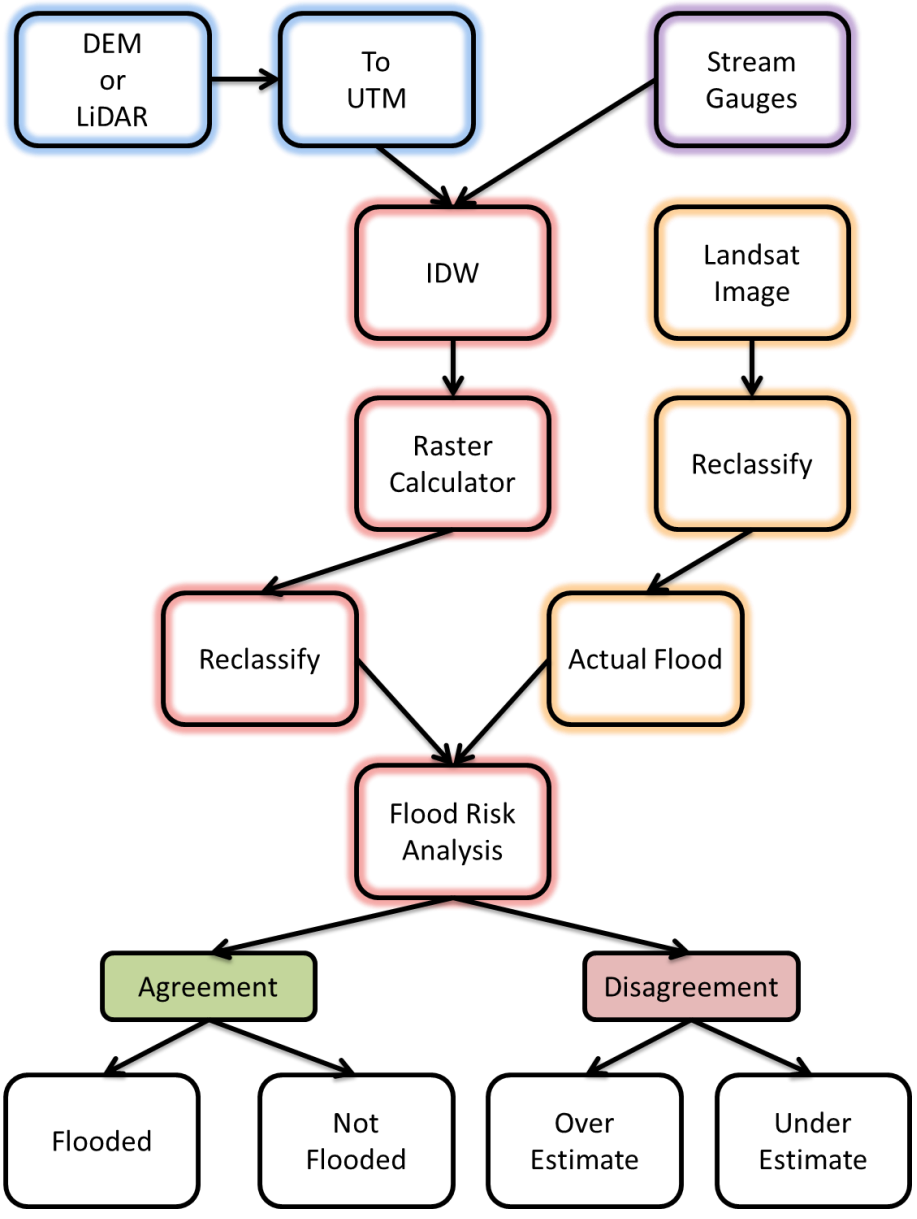

Figure 4: Flow chart of the methodology used to develop the flood risk model.

DEMs were obtained for study area in different resolutions – 30m, 10m, and 1m – or the native resolution of 1 arc second, 1/3 arc second, and 1/9 arc second, respectively. Prior to spatially analyzing the data layers, the coordinate systems of the different layers were converted to a Universal Transverse Mercator (UTM) projected coordinate system in order to do the analysis in meters rather than in decimal degrees. This was done to minimize areal distortion from the map projection for the area calculations. Four separate 30m DEM files, eight separate 10m DEM files, and 16 separate 1m LiDAR DEM files were downloaded from the USGS National Map Viewer and mosaicked into one seamless DEM.

The National Weather Services (NWS) has pre-defined longitude and latitude coordinates for the stream gauges for the Illinois River. The day of the flood event of was April 23rd, 2013. However, the water level of was derived from the hydrograph provided by NWS for each stream gauge for the same date used in the accuracy assessment Landsat Imagery, April 29th, 2013. The data were inserted into an Excel sheet along with the name, longitude and latitude of each stream gauge. Five different Excel files were created to accommodate the different stream gauge distribution scenarios. Then, the files were imported into ArcMap and plotted as point data.

Before simulating the flood risk analysis maps, the Landsat 8 OLI imagery for the study area – collected 2013/4/29 – was acquired from the USGS Global Visualization Viewer (GLOVIS) and multiple images were merged into a single image, in order to generate an actual flood extent map. Then, it was reclassified using supervised classification (where the user creates "training sites" to specify the desired land cover

classes) to determine all the sites on the image that were water as well as those that were not water. Then, only the water associated with the Illinois River, which in this case is the actual water pixels on the day of interest, was isolated from the Landsat reclassified imagery. This was then converted to a polygon layer. After that, the desired stream gauges distribution and DEM resolution were added to the map document. The working environment in the GIS software was set so that the results would have the same extent of the Illinois River portion used in this study, and to have the same cell size of the desired DEM resolution (30,30 – 10,10 – 1,1).

Adapting Landsat Imagery to Study Area

The Landsat imagery that was used for accuracy assessment of each flood risk simulation was a Landsat 8 OLI image that was captured on April 29th of 2013 with a spatial resolution of 30 by 30 meters (USGS, 2014). The acquired Landsat imagery tiles (Figure 5) for the entire study area extent were captured on different days, which, based on water level, would result in errors in simulating. The Landsat 8 OLI imagery date for the central and north-eastern portions of the study area was dated April 29th, 2013. However, the south-western portion's closest date to the flood was April 20th, which is three days before the flood (Figure 5). Furthermore, the April 20th imagery had over 33% cloud coverage which would have increased error in the image classification.

While the simulation was conducted on the entire study area extent, the accuracy assessment was conducted only on the portion that matched the extent of the Landsat imagery obtained from April 29th, 2013. Since this may affect the results of the

simulation's accuracy assessment, future study should be conducted on an area that is completely covered with Landsat imagery of the same date.

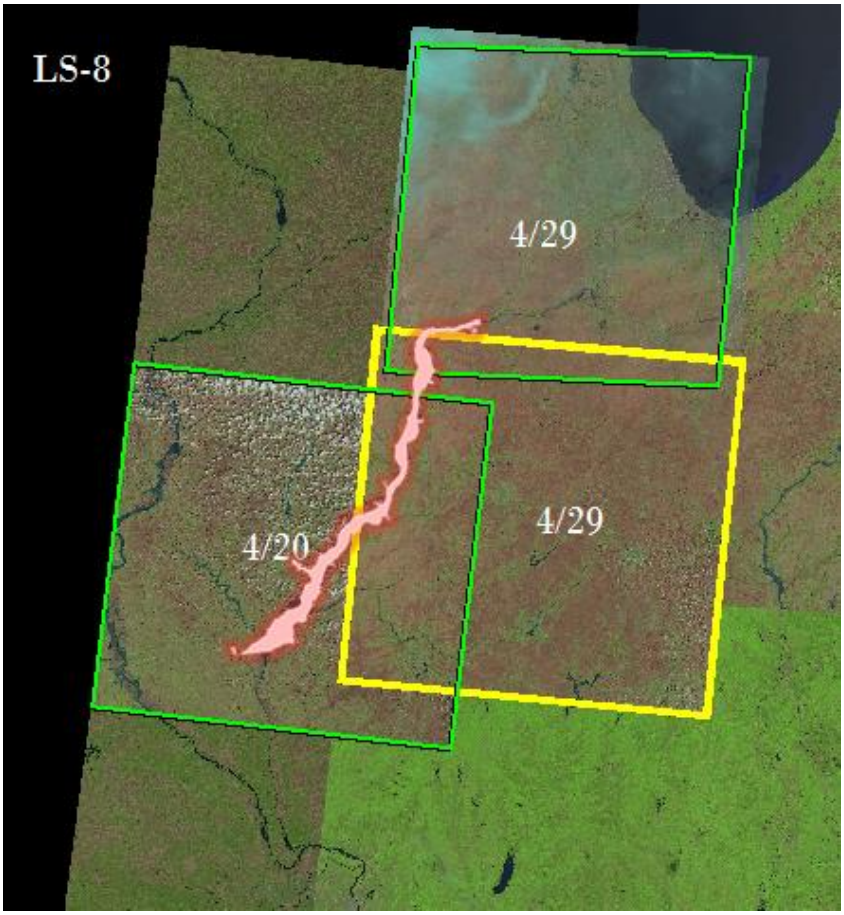

Figure 5: Landsat 8 OLI imagery as they appear on GLOVIS (Feb, 2014). The study area is shaded in red

Simulation Procedure

A series of raster-based GIS analysis procedures were used to predict the areas affected by the flood. Raster surfaces were interpolated at each DEM resolution from the stream gauge points using an inverse distance weighted (IDW) technique. The IDW

interpolation determines cell values using a linearly weighted combination of a set of sample points. This method assumes that the modeled variable loses influence the farther it is from its source (Watson et al., 1985). This was used to predict water levels at a particular flood stage in between points of known water levels along the river where gauges are absent.

Next, the Map Algebra Raster Calculator tool was used to predict inundation to the different DEM resolutions with the different stream gauges distributions. This was done using an expression that subtracts the IDW results from the desired DEM. This gives a flood prediction based on the stream gauge information where any positive value is **Flooded**, while any negative value is **Not Flooded**. In order to make the raster calculator results easier to compare, the results were reclassified using the Spatial Analyst Reclassify tool.

Generating Comparable Results

In order to perform a comparison between the actual flood (Landsat-based classification) and the projected inundation from the DEM, Landsat imagery was reclassified so that water was given the numerical value of "10" and no-water was given the value of "0". The map algebra results also were reclassified into two groups. Since the negative values indicate areas that are not affected by the interpolation, these areas were also given the value of "0" to indicate not flooded areas. In addition, the rest of the positive values were given the value of "1" to indicate flooded areas.

Lastly, the two layers were compared to determine the agreement in flooded/not flooded area result by the different DEM resolutions by using an expression that simply adds the pixel values of the two mentioned reclassifications. This step is critically important since, according to the new values, when adding the two layers together the results will determine if it is an agreement or a disagreement. These results are shown in Table 1.

Table 1: Flood risk simulation results

Calculator Value	Landsat Imagery	Simulation Prediction	Result
00	Not Flooded	Not Flooded	Agreement
01	Not Flooded	Flooded	Overestimation
10	Flooded	Not Flooded	Underestimation
11	Flooded	Flooded	Agreement

Accordingly, polygons were derived for each of the disagreement cases, one to represent overestimation and one that represents underestimation.

The study uses five different stream gauges distribution (Figures 6-10). Each combination of gauges was used to interpolate a flood prediction at each of the three different DEM resolutions. This resulted in a total of fifteen different combinations. The distribution of the stream gauges to form the different stream gauges densities was selected to allow for a logical distribution. For instance, the two (2) stream gauges distribution used the second stream gauge from the northeast, as well as, from the southwest. This was done to avoid using the two in the edges or the two in the middle as this may skew the results, increasing total error.

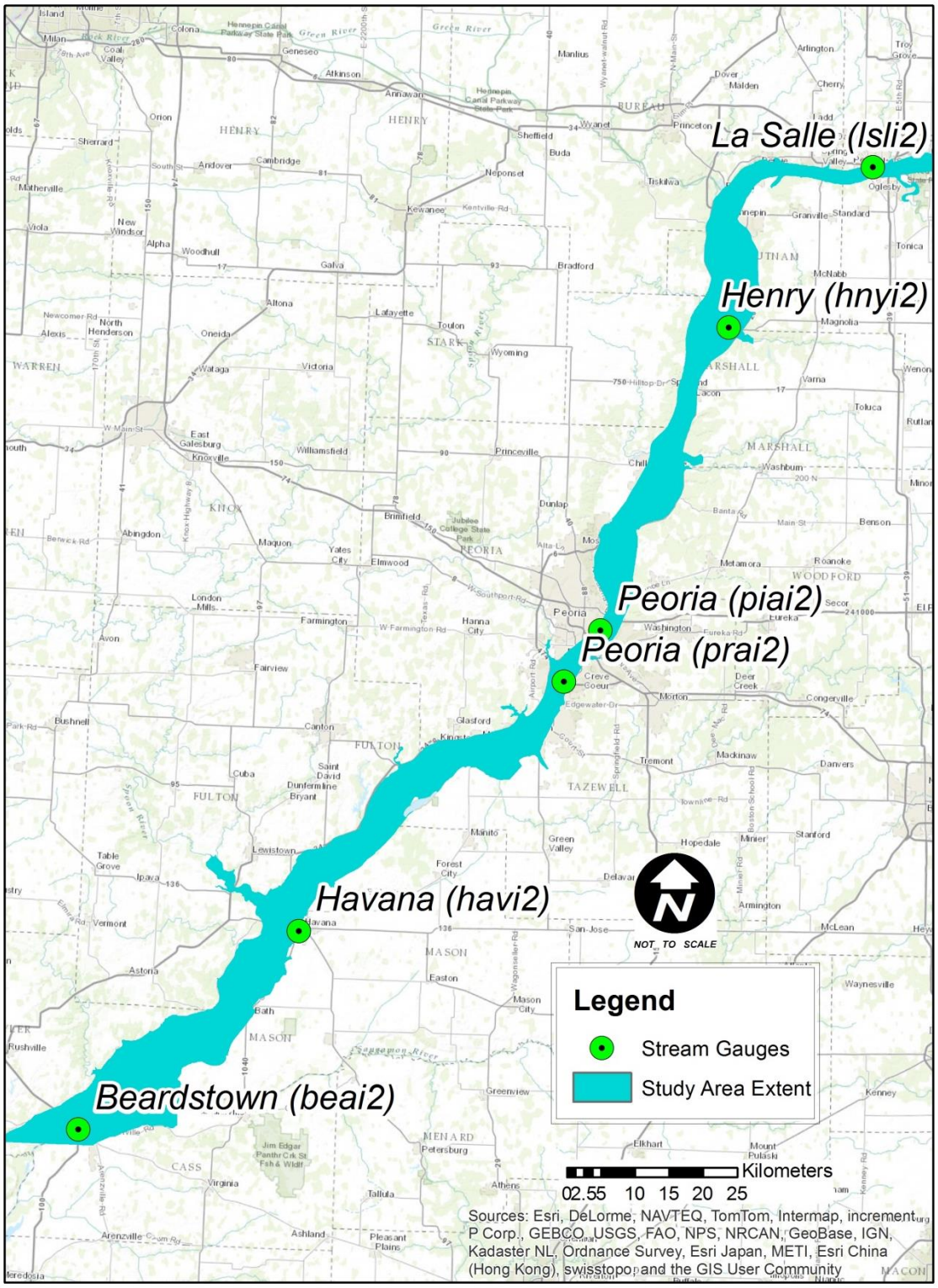

Figure 6: Distribution of stream gauges for six (6) gauges scenario

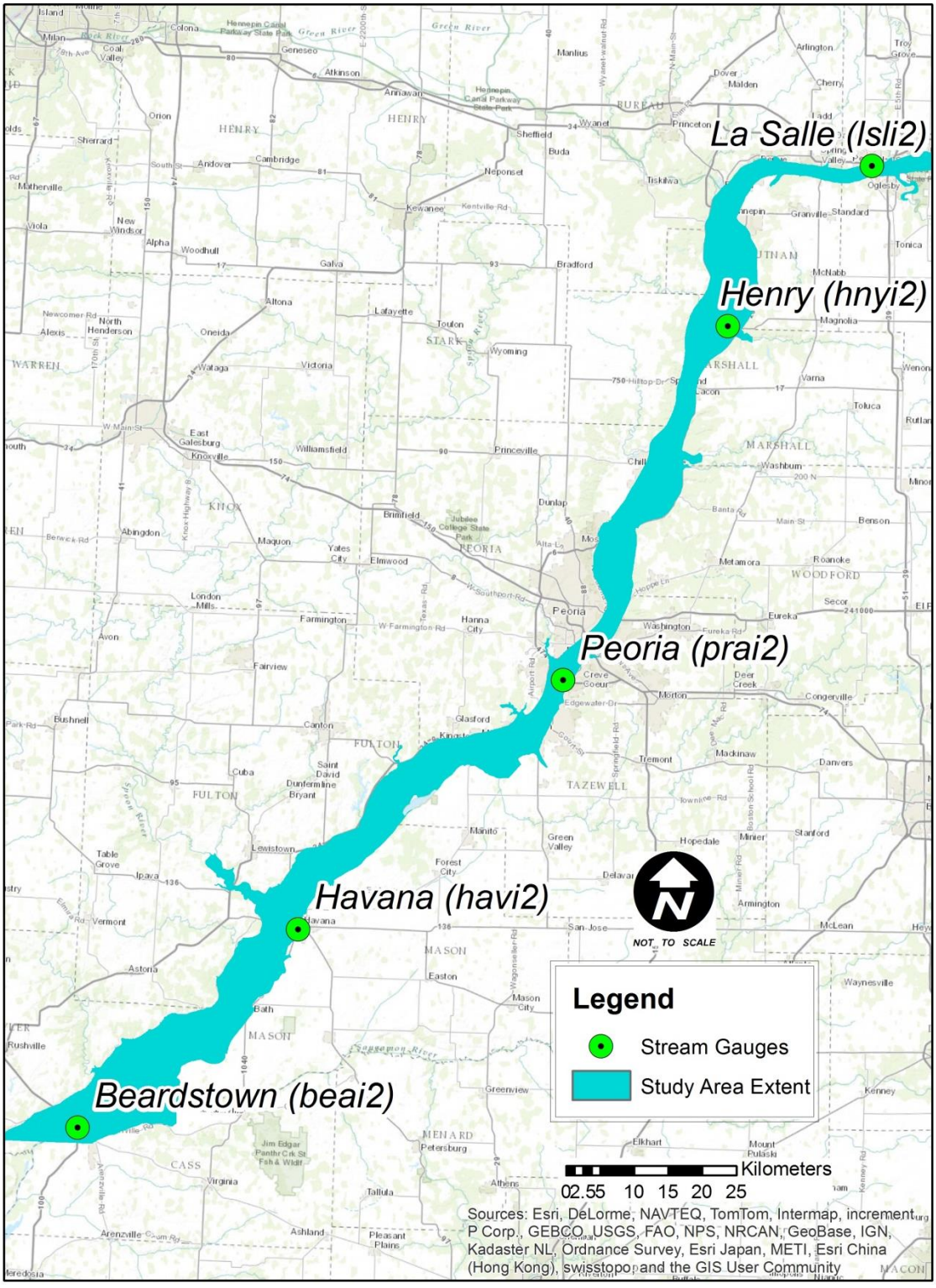

Figure 7: Distribution of stream gauges for five (5) gauges scenario

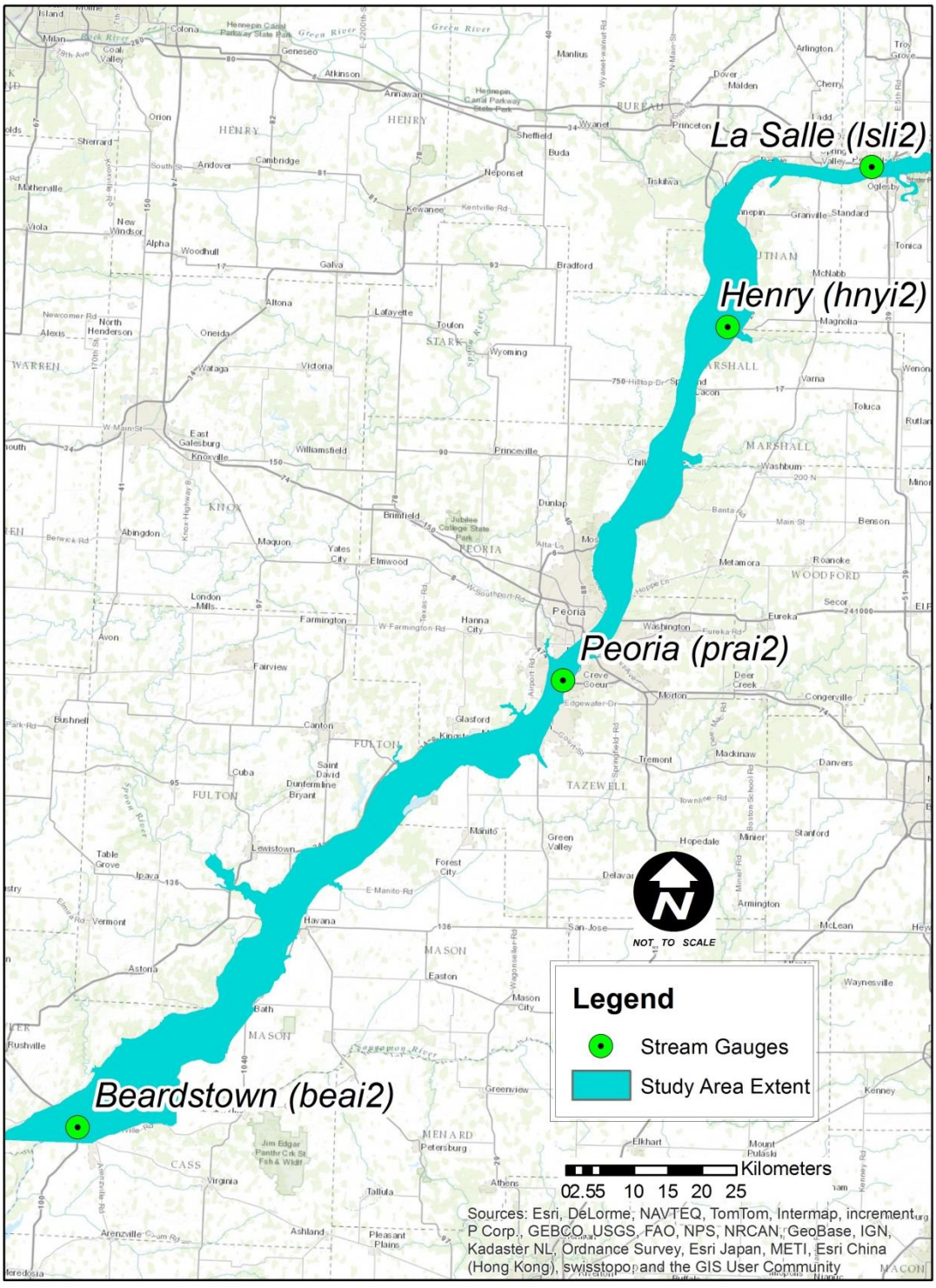

Figure 8: Distribution of stream gauges for four (4) gauges scenario

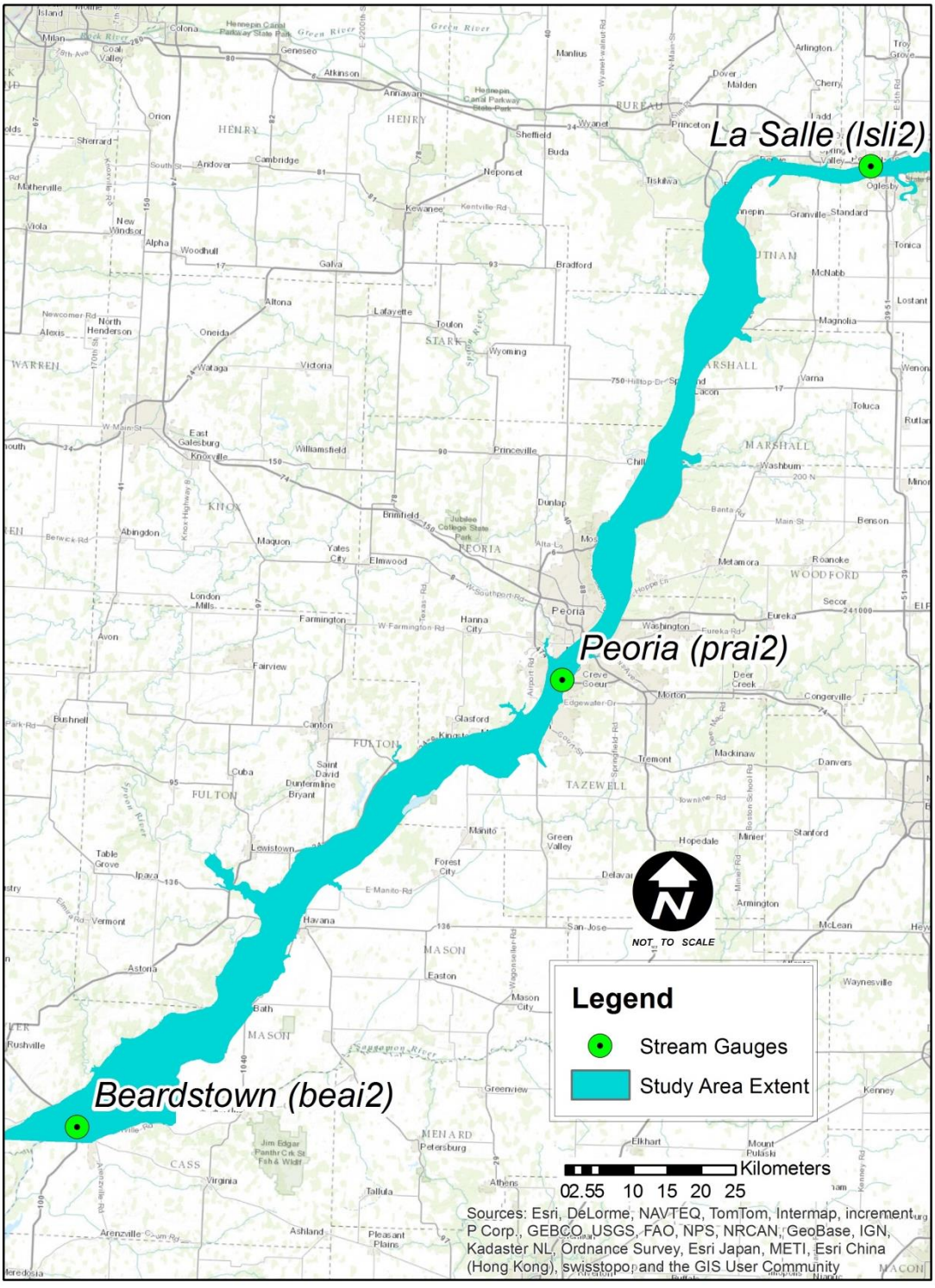

Figure 9: Distribution of stream gauges for three (3) gauges scenario

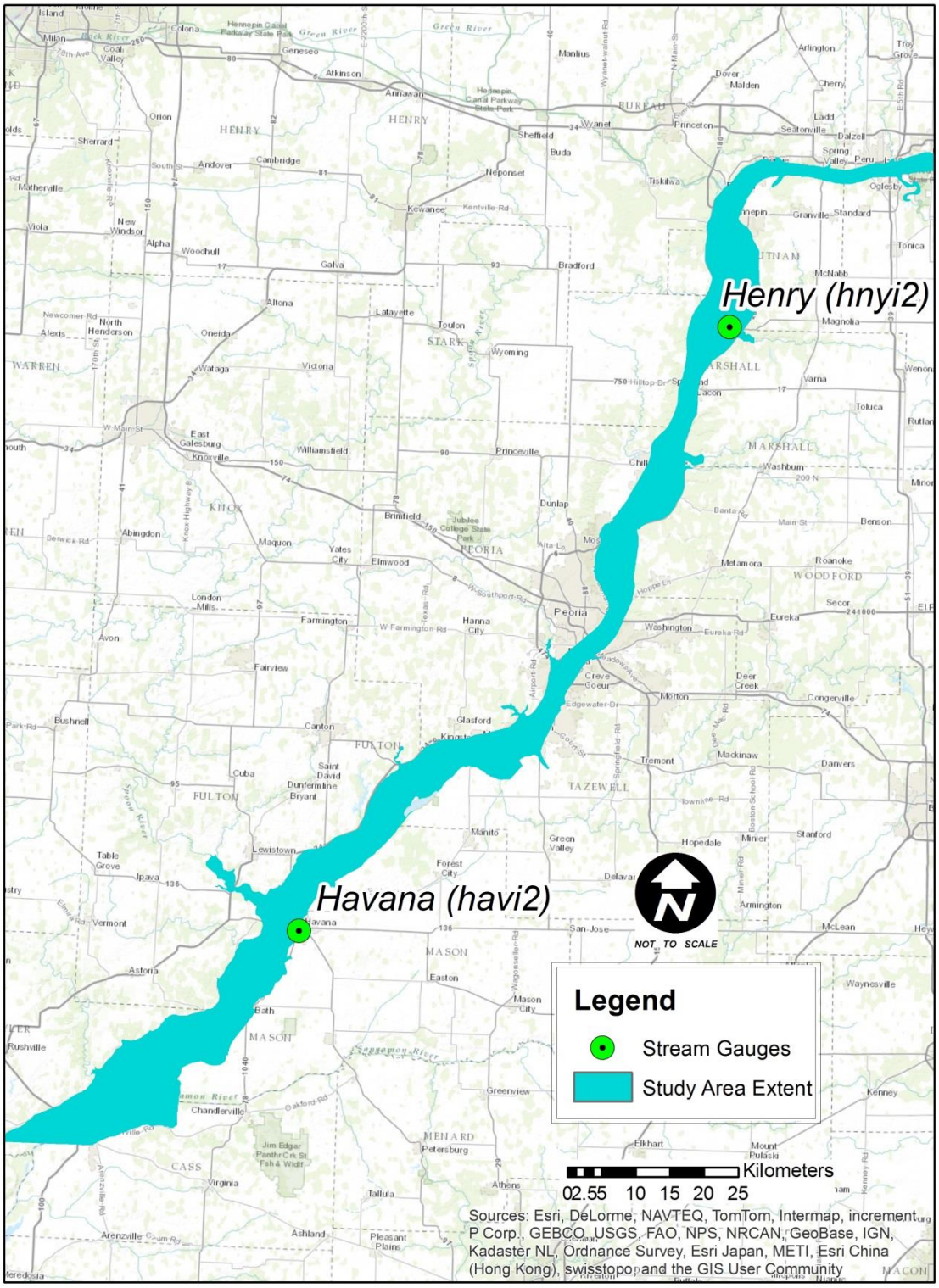

Figure 10: Distribution of stream gauges for two (2) gauges scenario

CHAPTER III

RESULTS

This study resulted in 15 comparisons between actual flooded areas and predicted inundation at three DEM resolutions and five stream gauge combinations. Each run resulted in a different ratio between the agreements (flooded and not flooded, in both actual and predicted) and the disagreements (overestimation and underestimation). Figures 11 – 25 show the resulted flood risk simulation maps for selected locations in the study area. In these maps the beige shaded area is where the simulated map agreed with the actual water map (which was derived from the Landsat imagery) on the **Not Flooded** areas. Likewise, the blue shaded area is the agreement on **Flooded** areas. The red and green shaded areas show disagreements with the actual water map, where the red areas show the **underestimation** of the model, and the green areas show the **overestimation**.

When visually comparing the extent of the predicted floods, there appears to be no significant difference between the different stream gauges distribution or between using different DEM resolution. Underestimation is seen across the edges of the river, while overestimation is clustered in the southwest end as well as the northeast end of the Illinois River. However, the two (2) stream gauges distribution scenario has the highest

error in all DEM resolutions, this maybe because most interpolation methods do not work well with less than 3 points.

Flood Risk Analysis maps with a 30m DEM Resolution

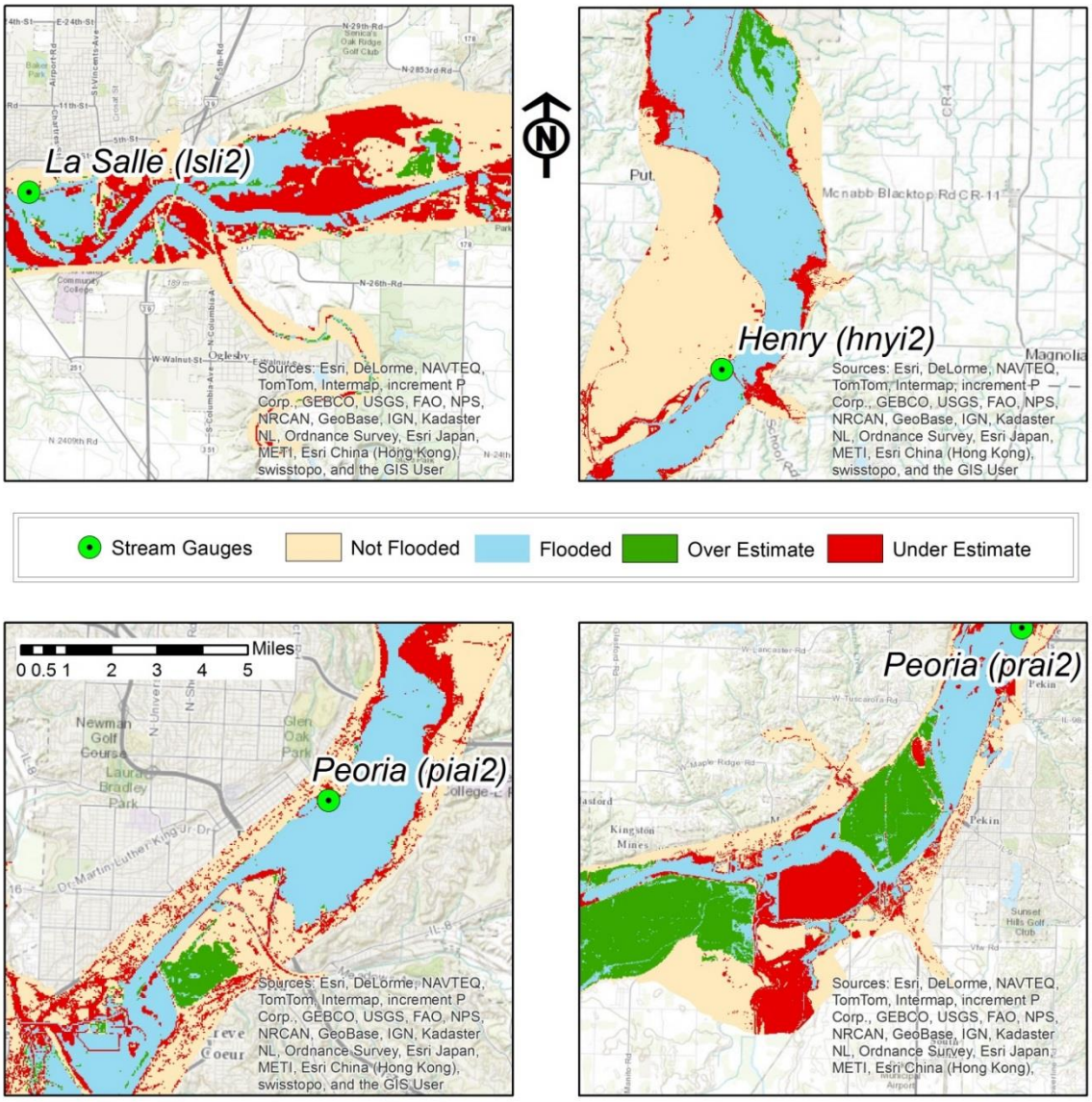

Figure 11: Flood risk simulation map for the 30m DEM, 6 stream gauges scenario. Refer to Figure 6 for stream gauges locations

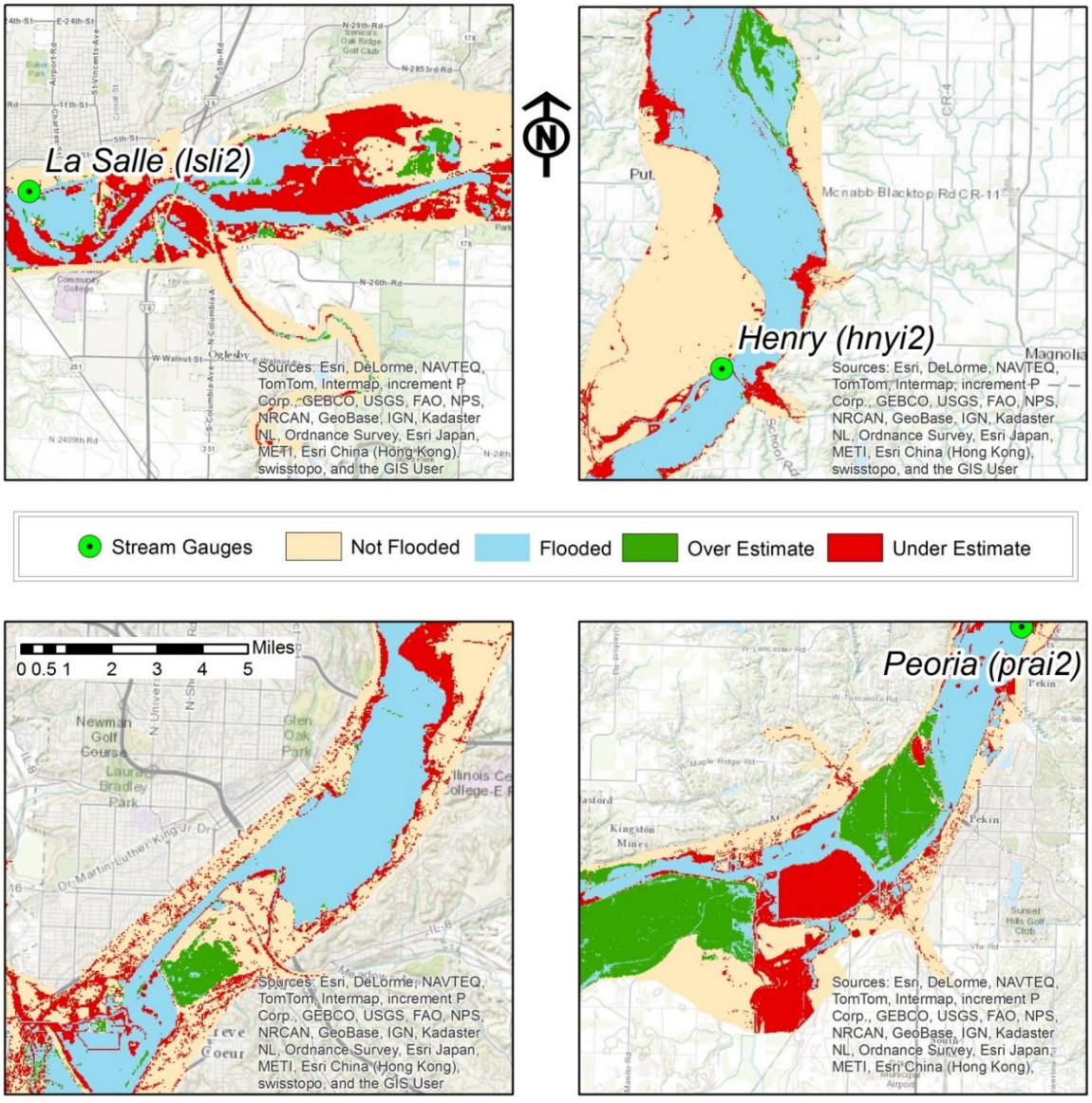

Figure 12: Flood risk simulation map for the 30m DEM, 5 stream gauges scenario. Refer to Figure 7 for stream gauges locations

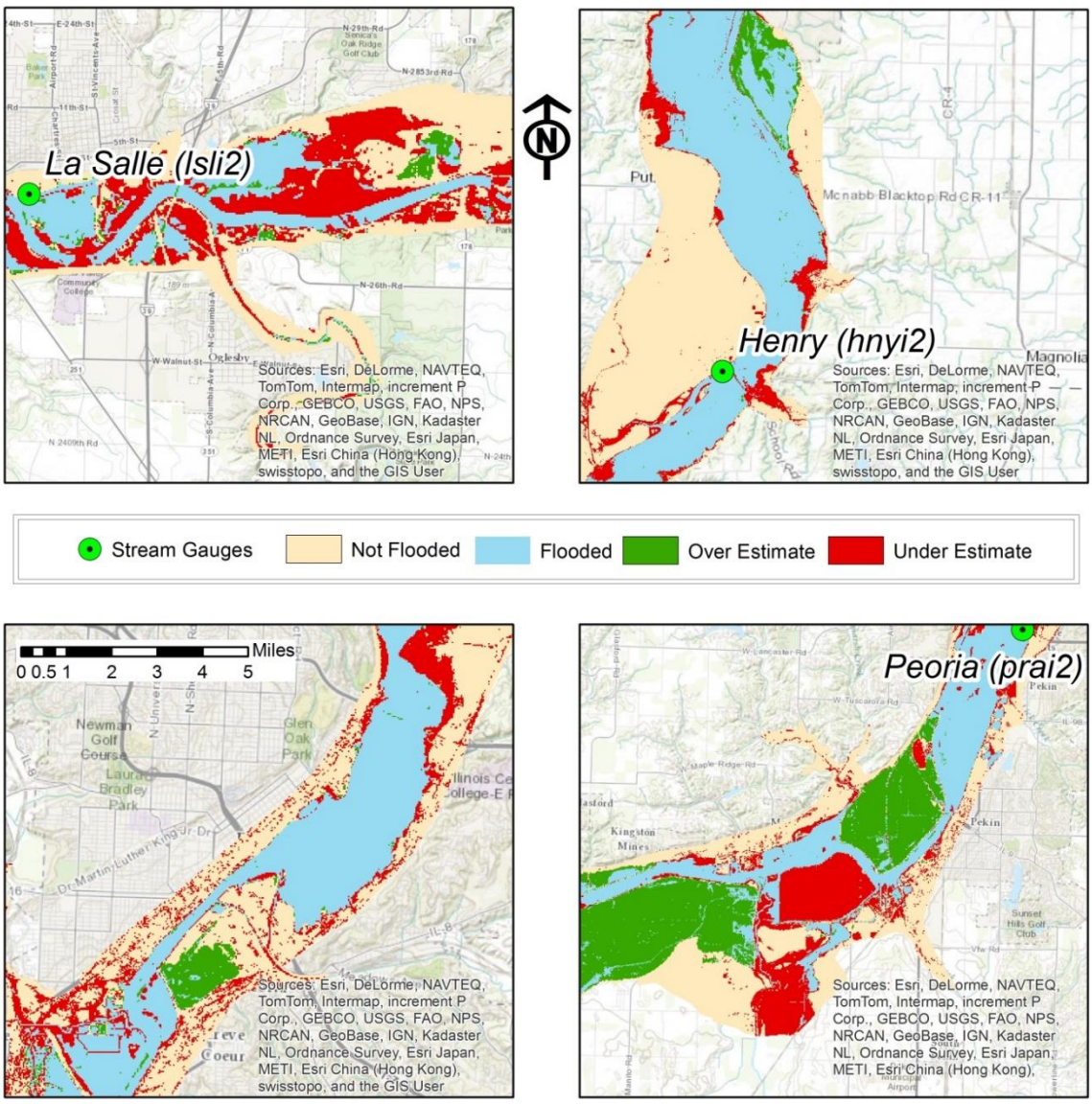

Figure 13: Flood risk simulation map for the 30m DEM, 4 stream gauges scenario. Refer to Figure 8 for stream gauges locations

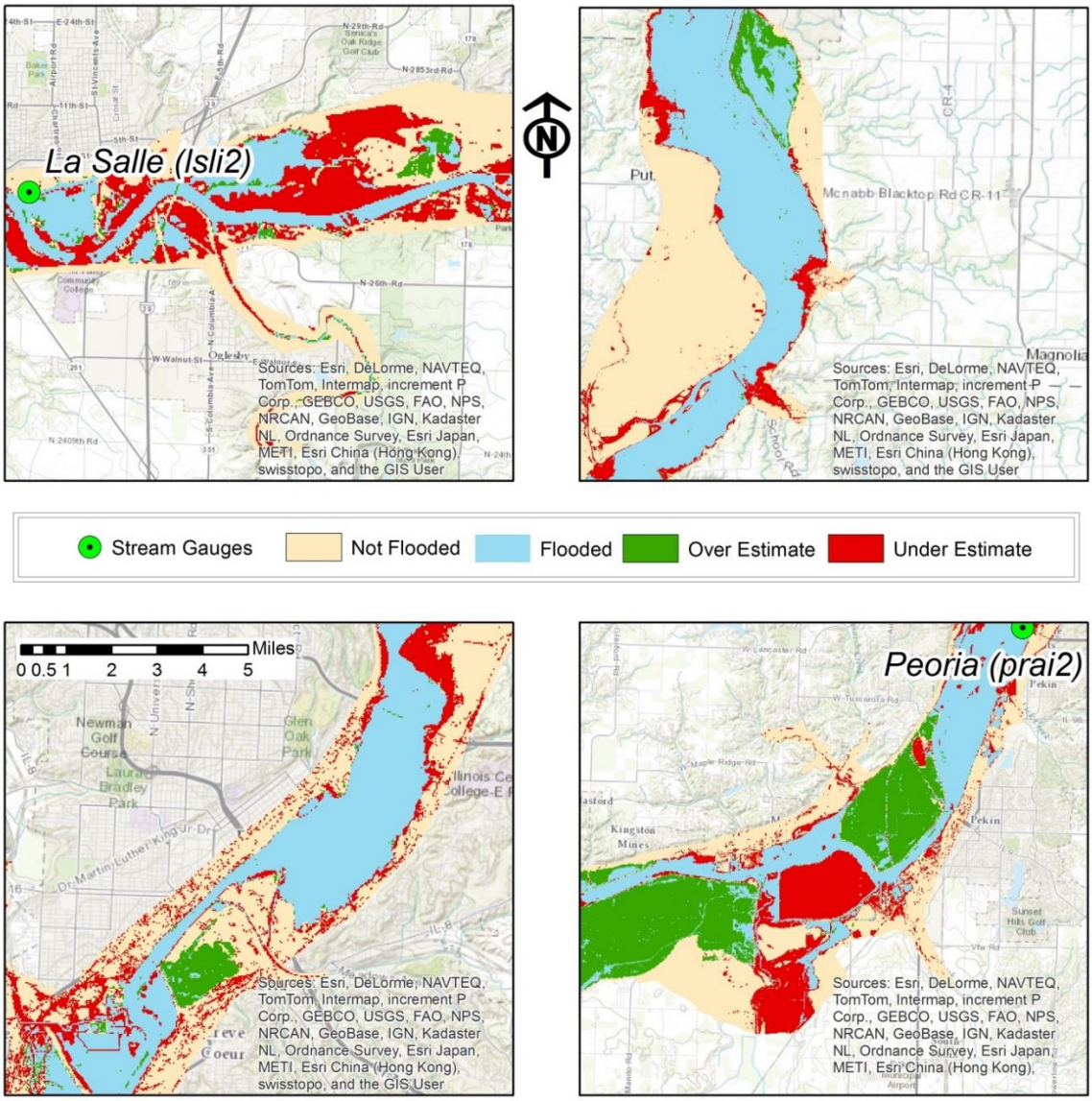

Figure 14: Flood risk simulation map for the 30m DEM, 3 stream gauges scenario. Refer to Figure 9 for stream gauges locations

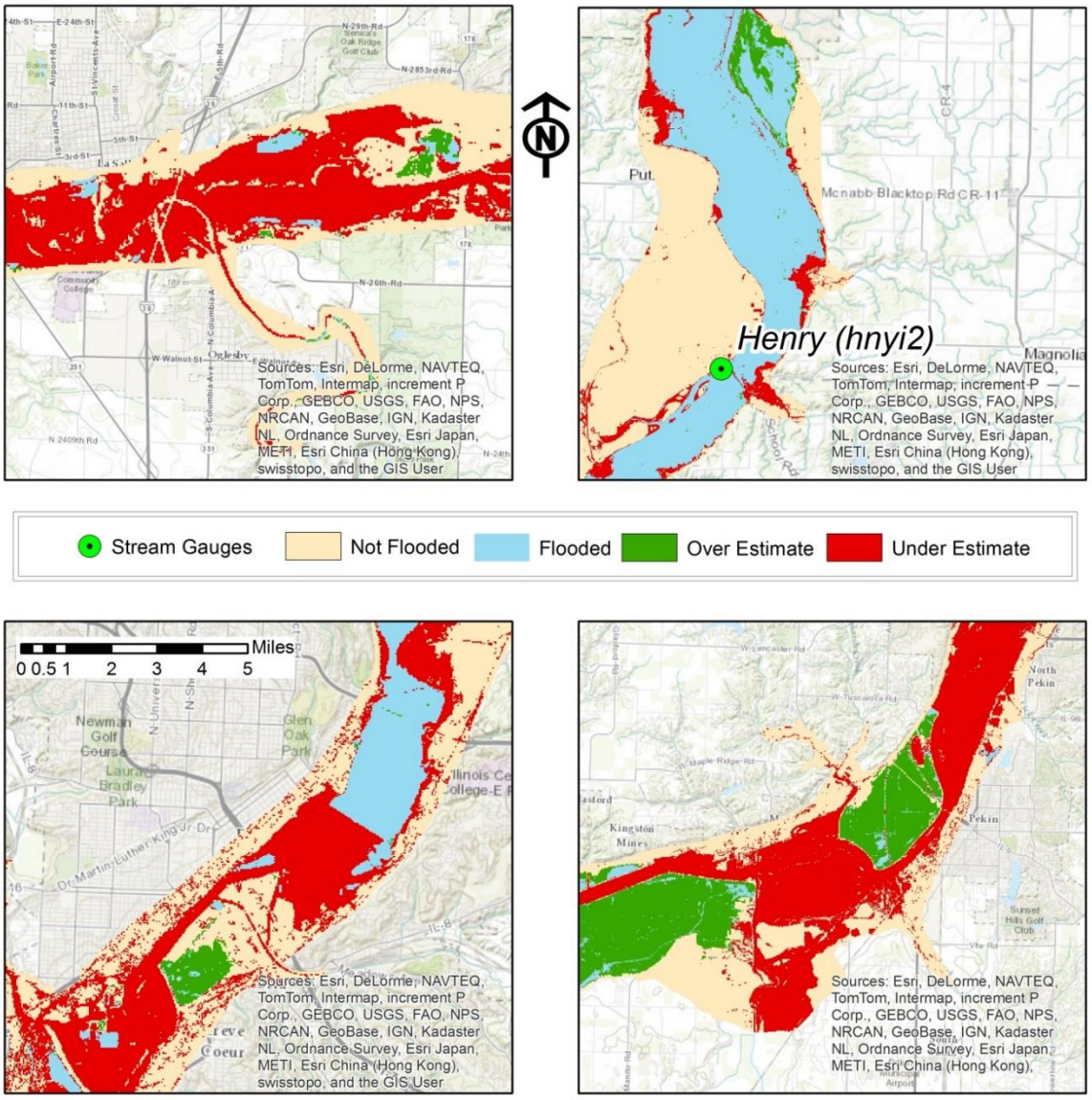

Figure 15: Flood risk simulation map for the 30m DEM, 2 stream gauges scenario. Refer to Figure 10 for stream gauges locations

Flood Risk Analysis maps with a 10m DEM Resolution

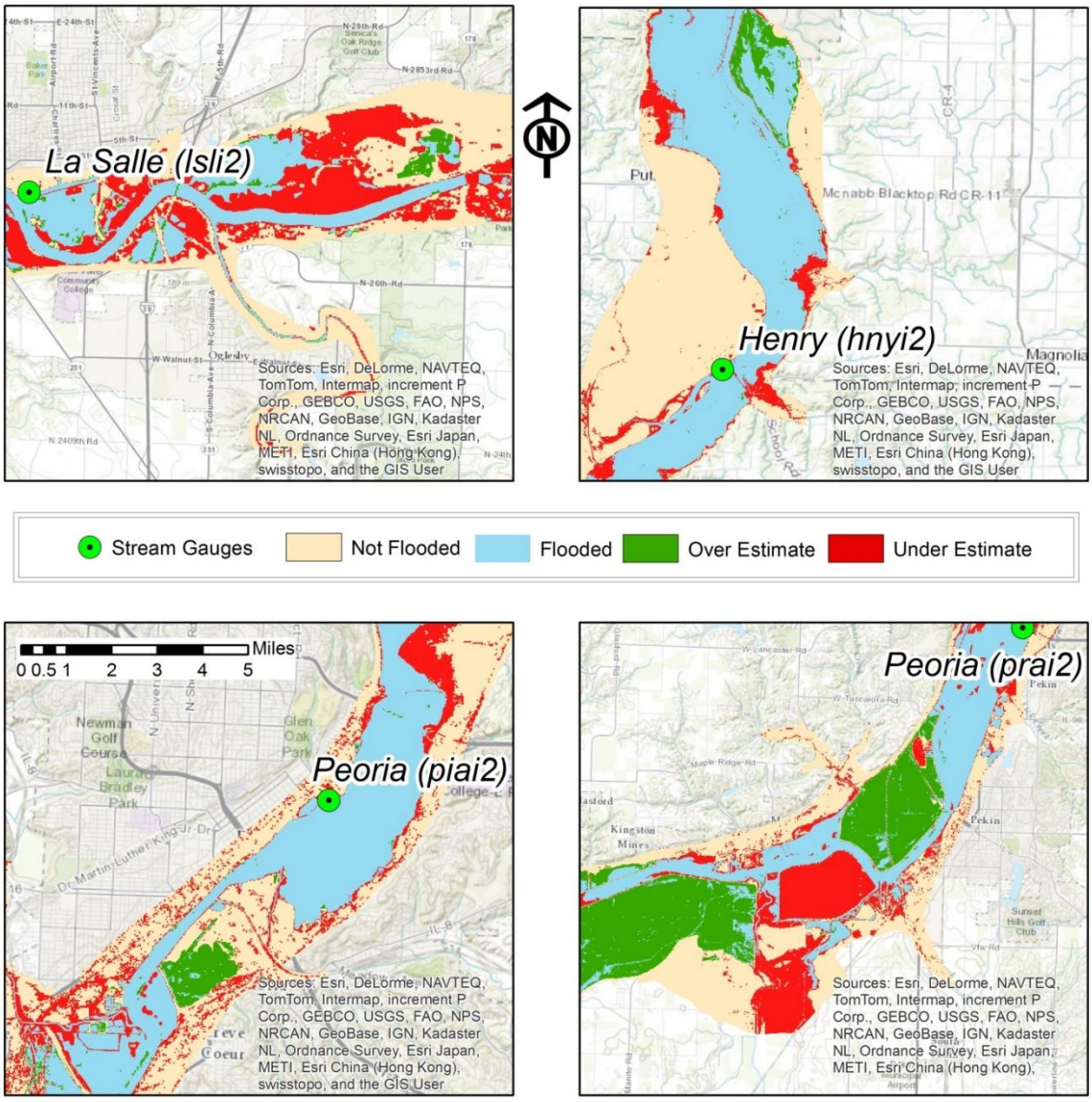

Figure 16: Flood risk simulation map for the 10m DEM, 6 stream gauges scenario. Refer to Figure 6 for stream gauges locations

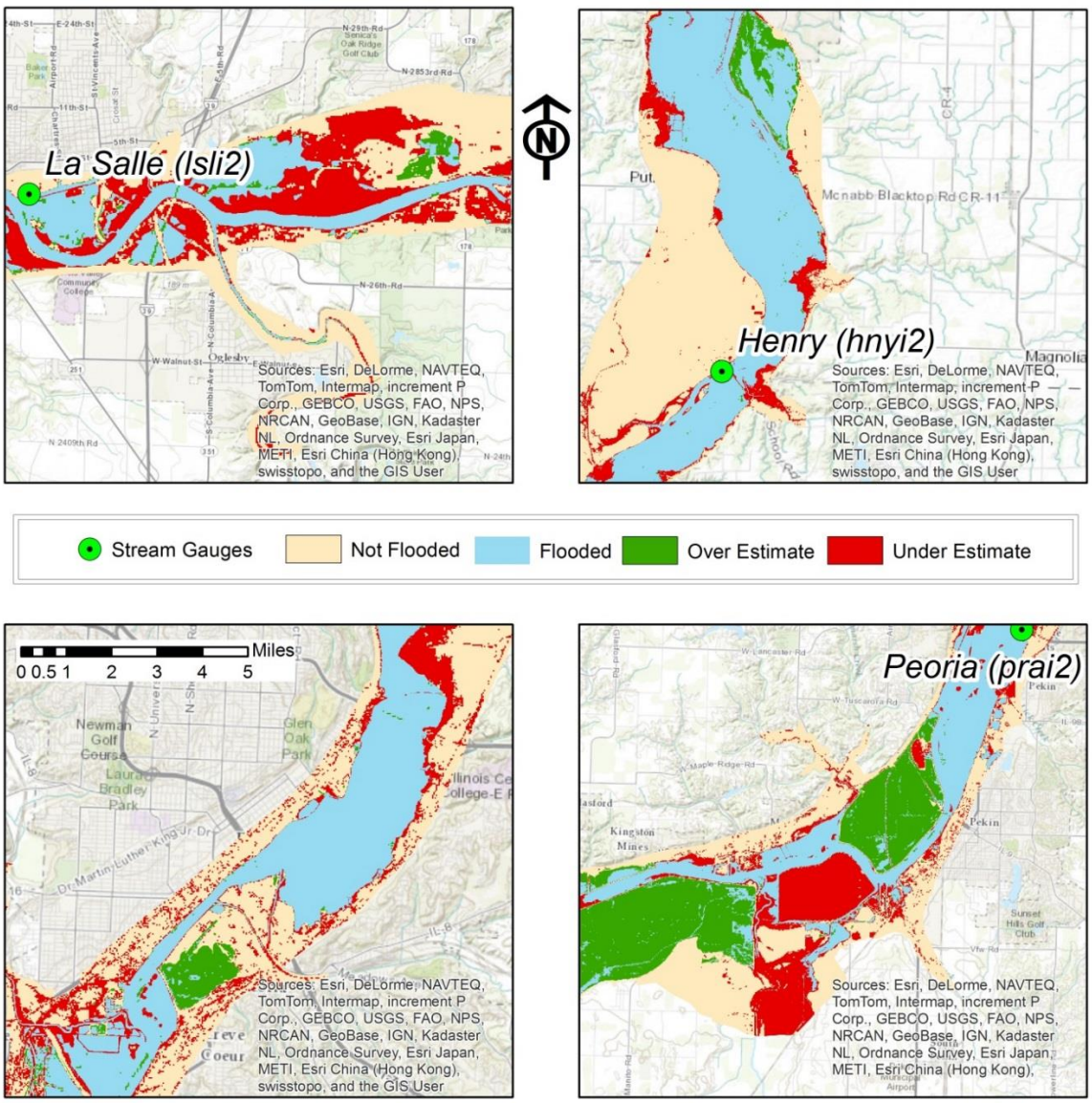

Figure 17: Flood risk simulation map for the 10m DEM, 5 stream gauges scenario. Refer to Figure 7 for stream gauges locations

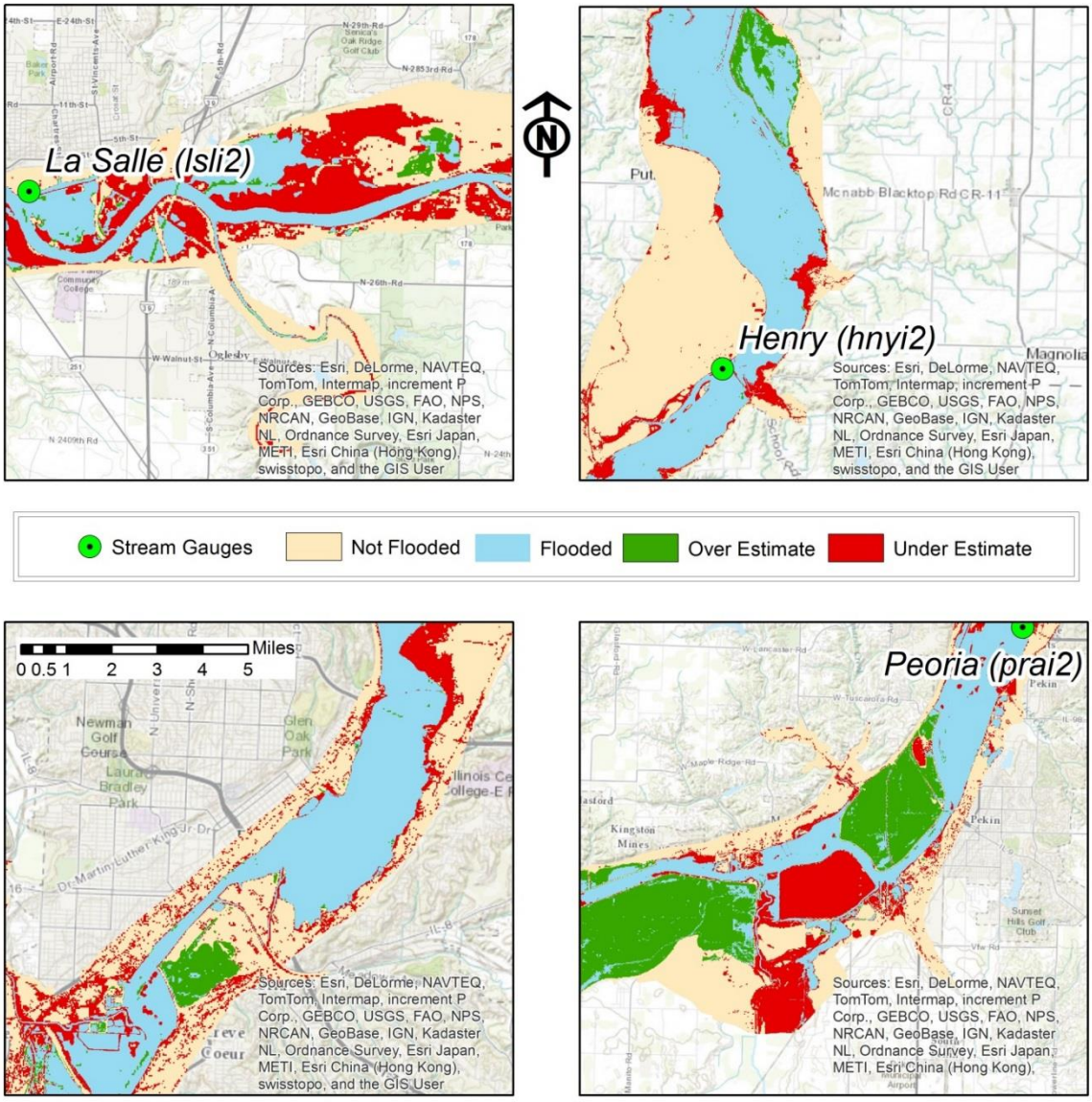

Figure 18: Flood risk simulation map for the 10m DEM, 4 stream gauges scenario. Refer to Figure 8 for stream gauges locations

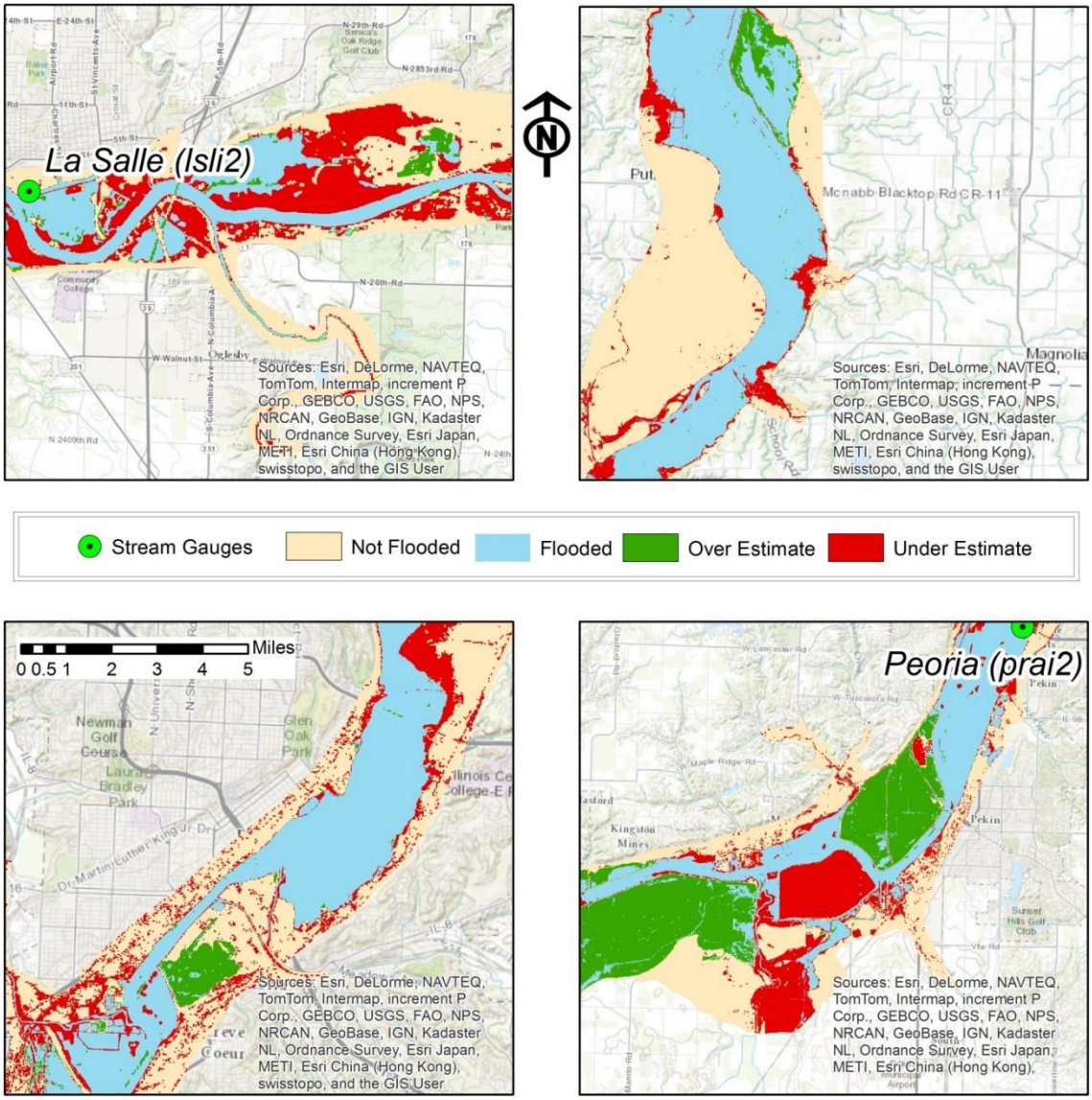

Figure 19: Flood risk simulation map for the 10m DEM, 3 stream gauges scenario. Refer to Figure 9 for stream gauges locations

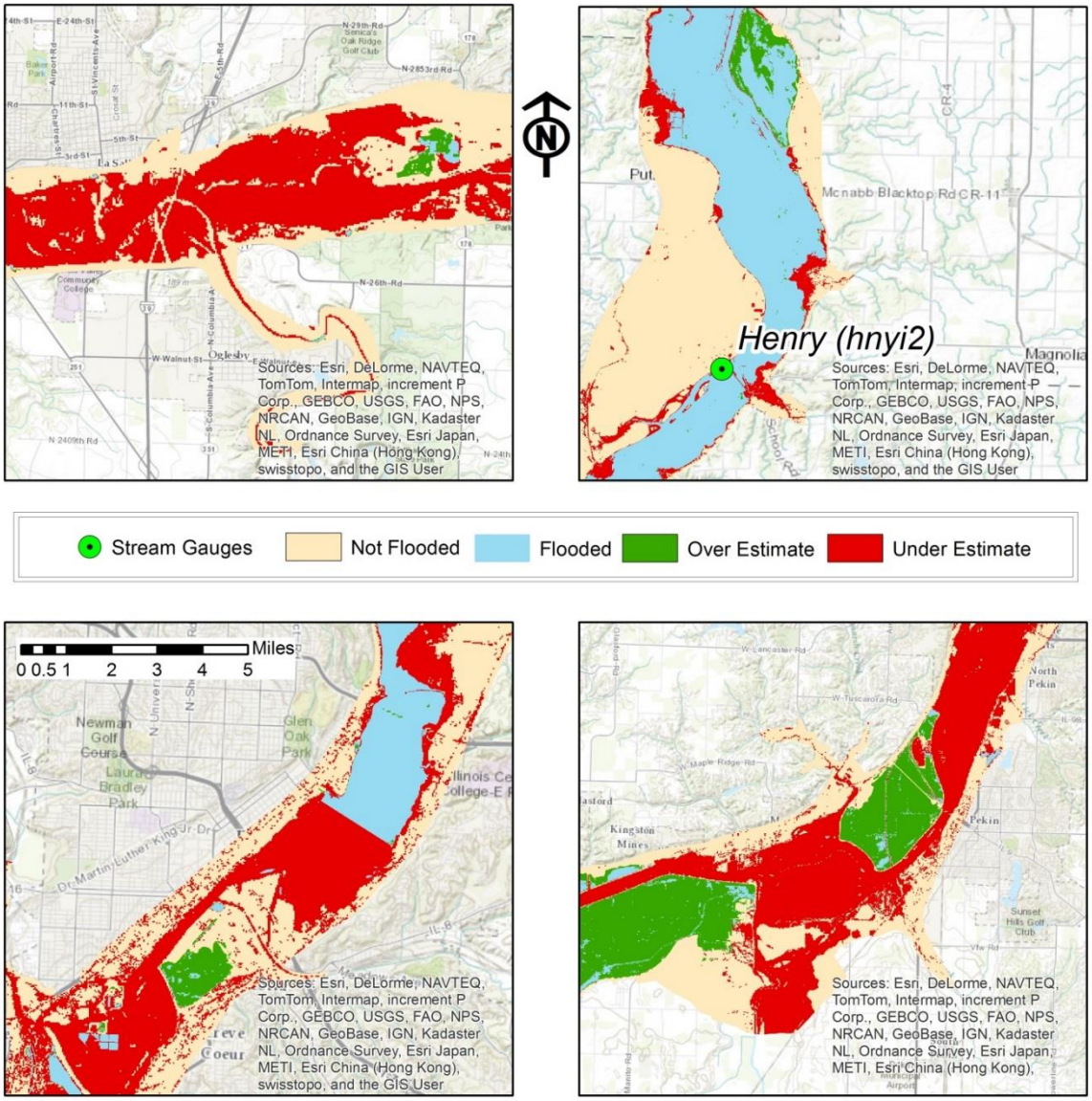

Figure 20: Flood risk simulation map for the 10m DEM, 2 stream gauges scenario. Refer to Figure 10 for stream gauges locations

Flood Risk Analysis maps with a 1m DEM Resolution

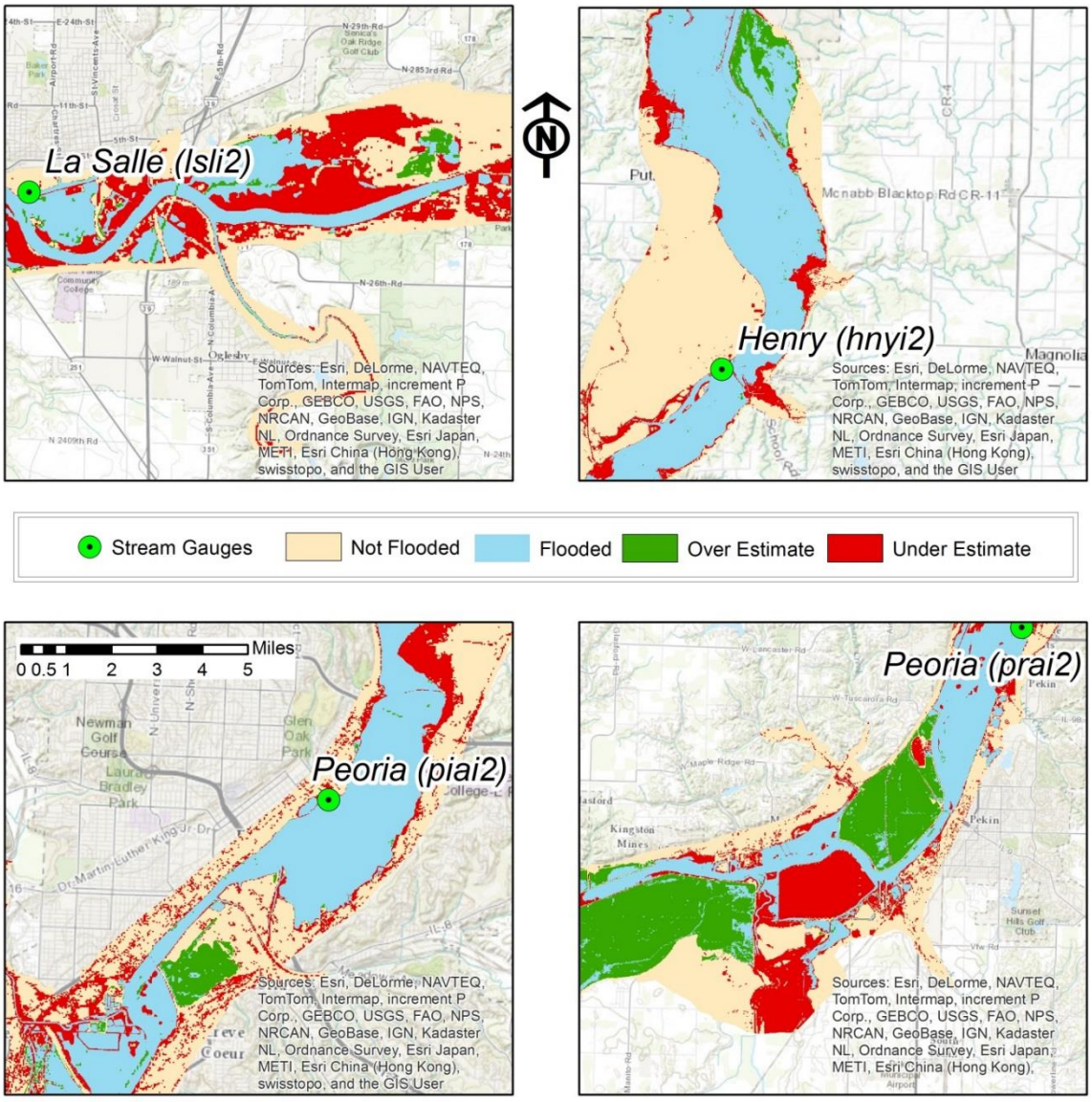

Figure 21: Flood risk simulation map for the 1m DEM, 6 stream gauges scenario. Refer to Figure 6 for stream gauges locations

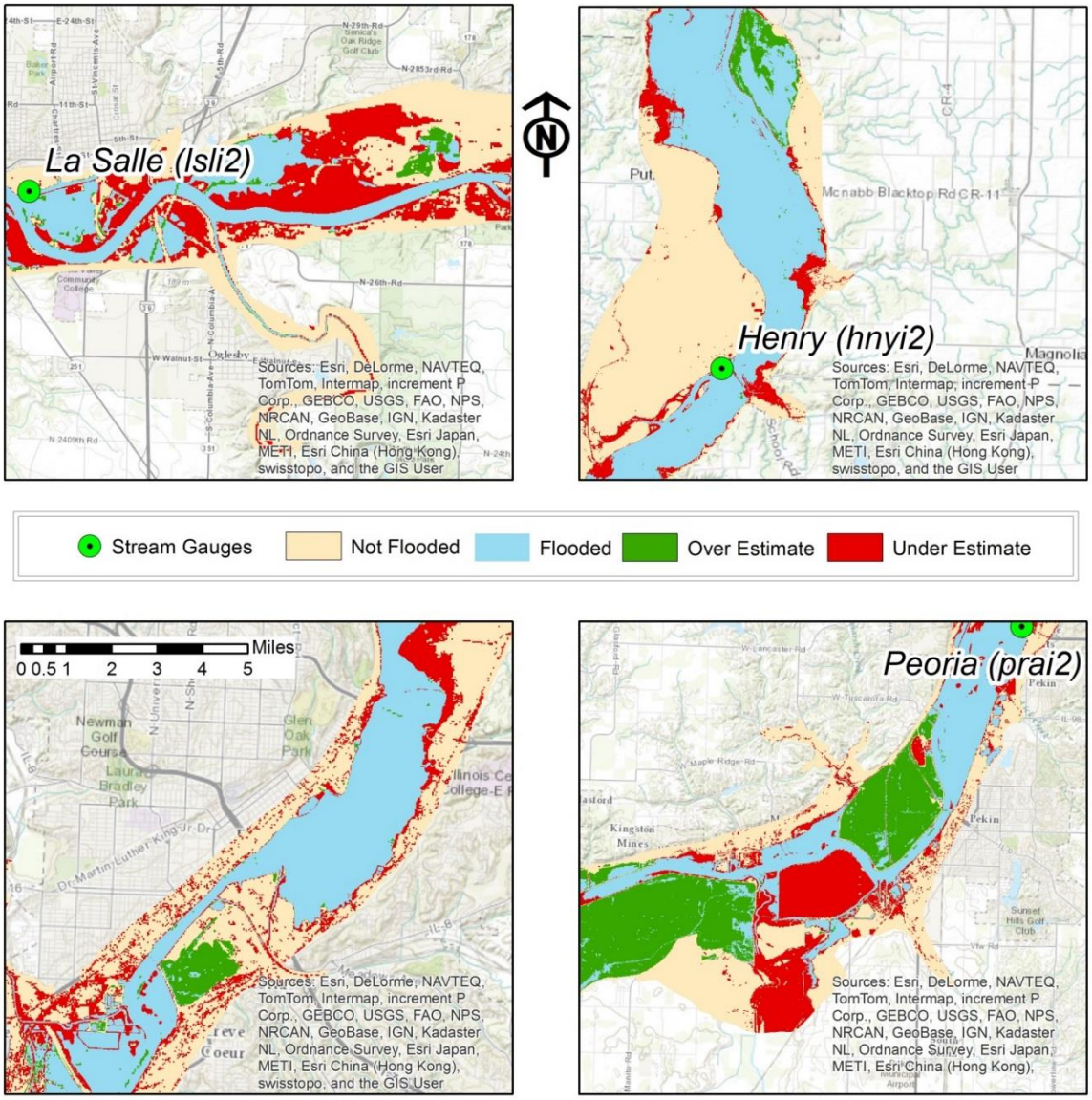

Figure 22: Flood risk simulation map for the 1m DEM, 5 stream gauges scenario. Refer to Figure 7 for stream gauges locations

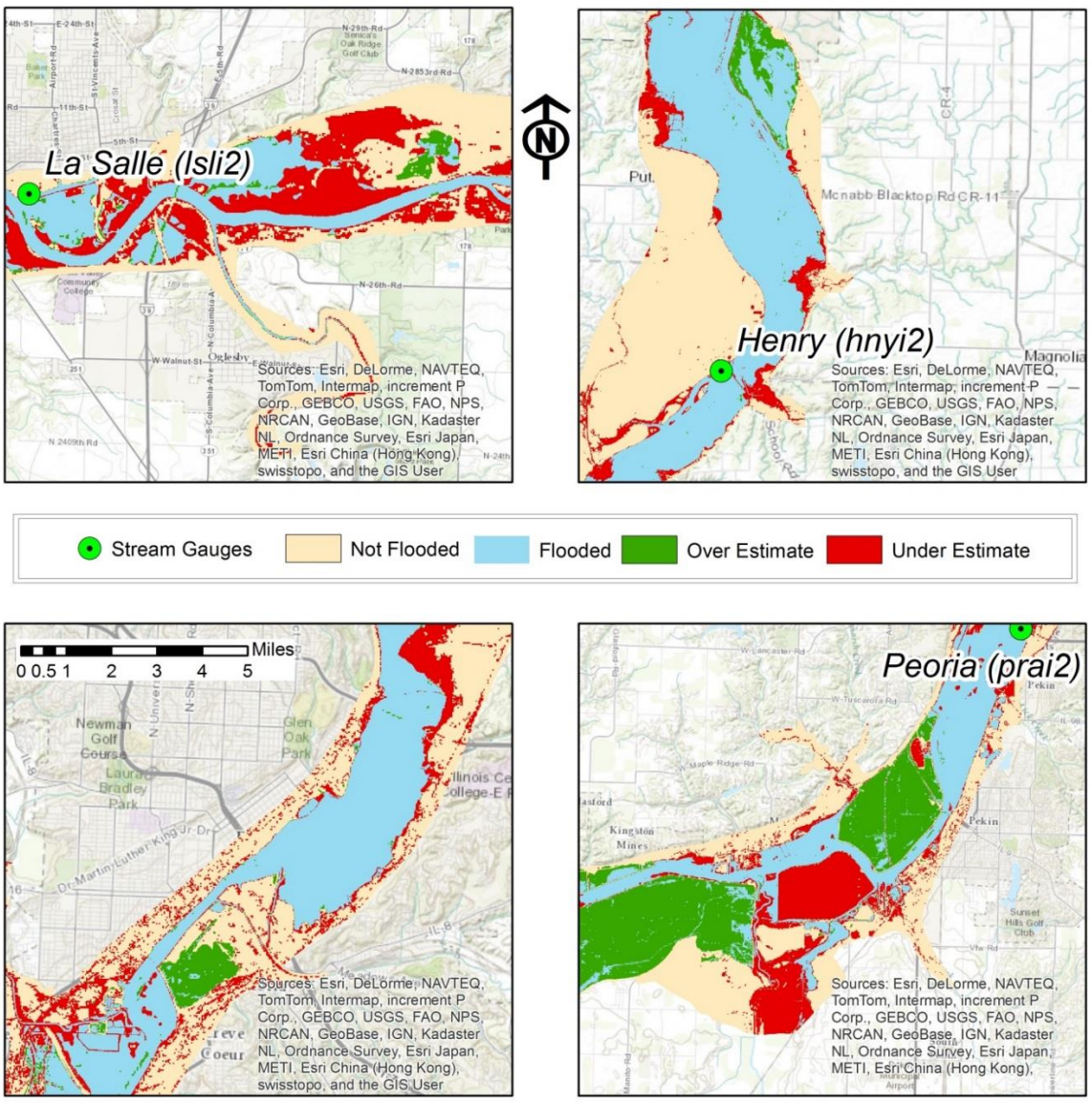

Figure 23: Flood risk simulation map for the 1m DEM, 4 stream gauges scenario. Refer to Figure 8 for stream gauges locations

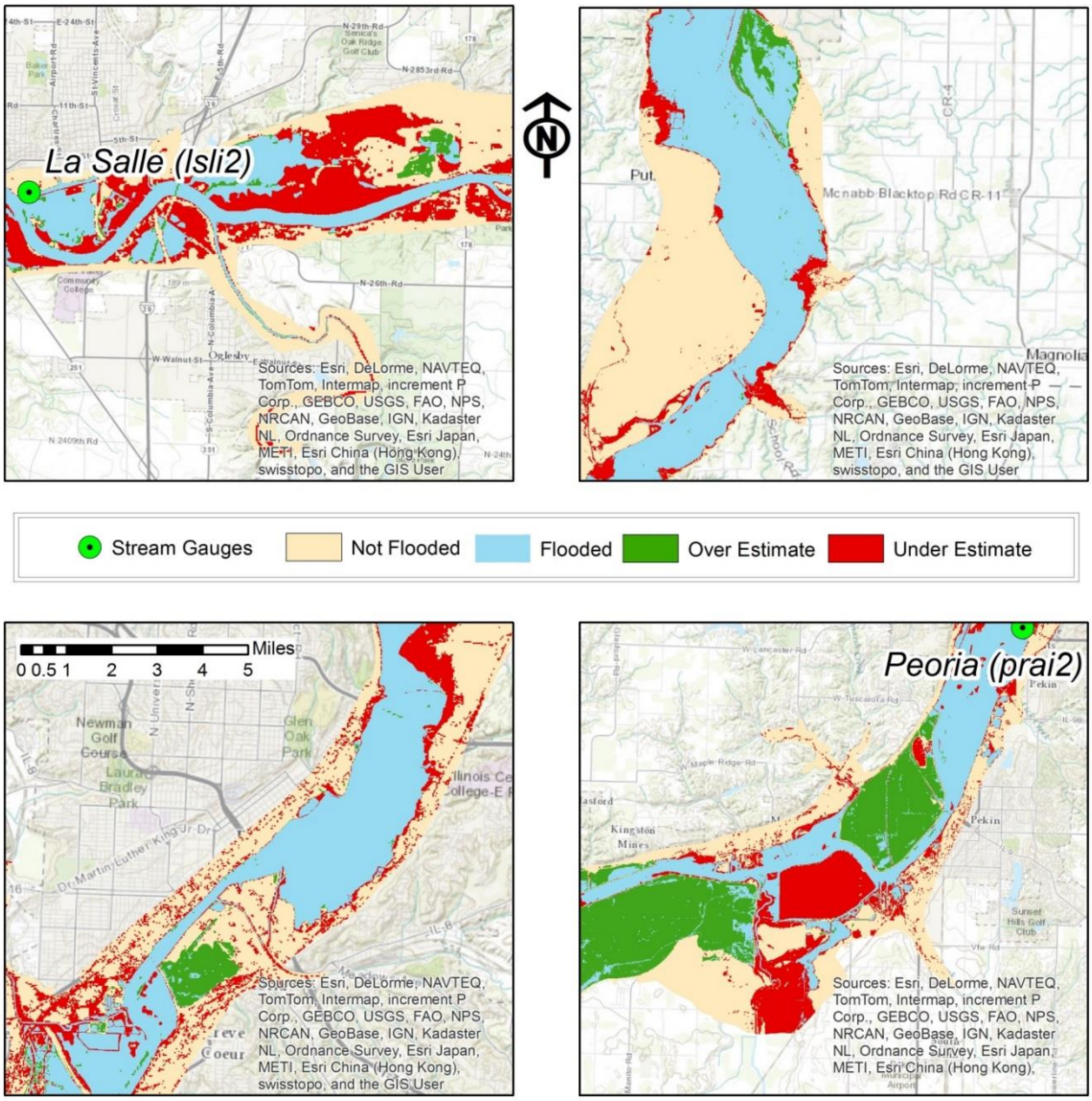

Figure 24: Flood risk simulation map for the 1m DEM, 3 stream gauges scenario. Refer to Figure 9 for stream gauges locations

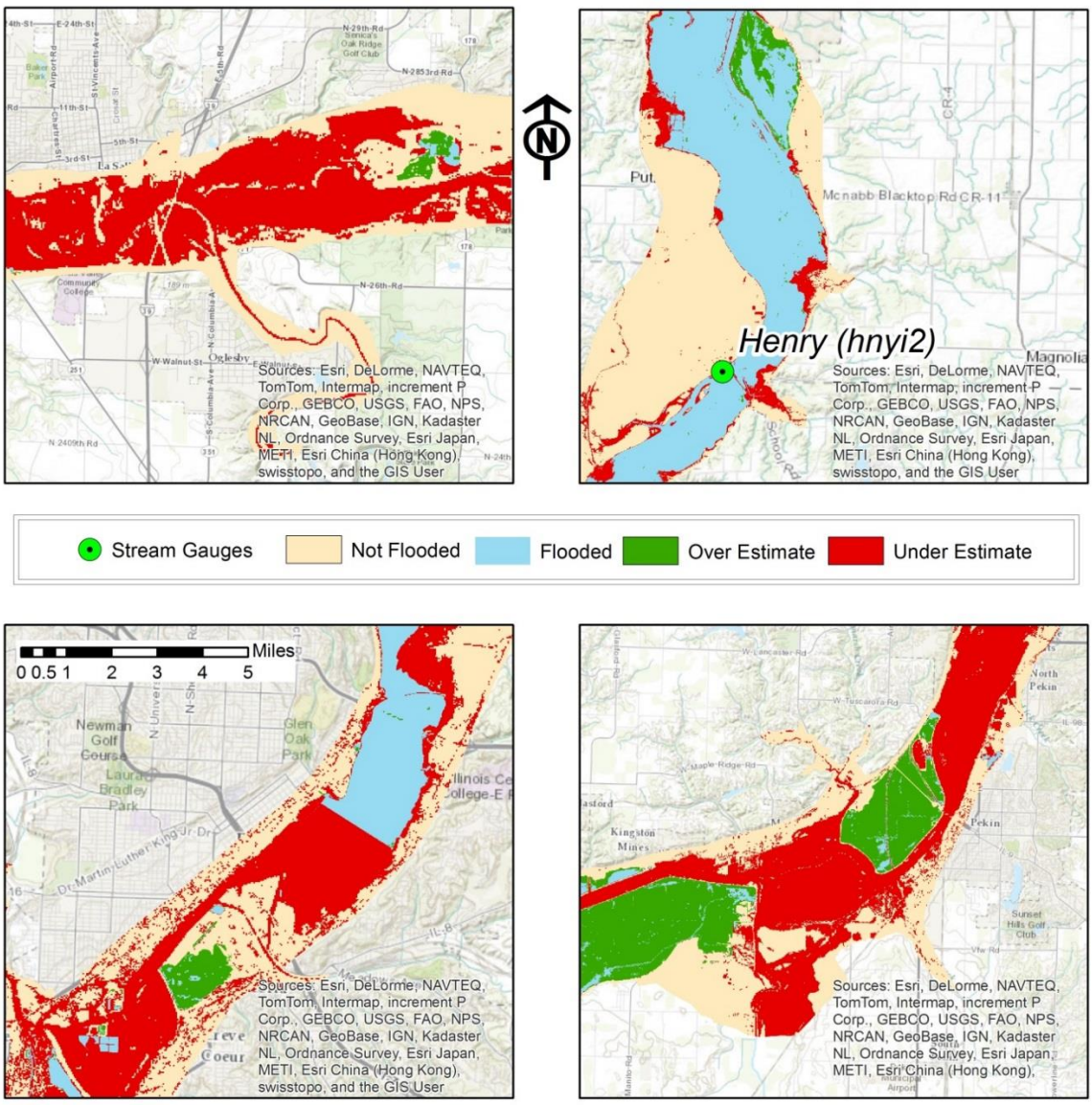

Figure 25: Flood risk simulation map for the 1m DEM, 2 stream gauges scenario. Refer to Figure 10 for stream gauges locations

Since the disagreement of the model with the actual water map is what matters to compare, and since the variation between the different maps is not visually significant, actual areas of agreement and disagreement were computed (Table 2).

Table 2: Flood risk simulation disagreements in km^2 and error percentages

Total Area of Study Area			610.62 km^2			
DEM Resolution 30 m						
Number of Gauges	Over Estimate km^2	Over Estimate %	Under Estimate km^2	Under Estimate %	Total Disagreement km^2	Error Percentage %
2	53.42	8.75	127.92	20.95	181.36	29.70
3	58.83	9.63	78.97	12.93	137.80	22.57
4	58.84	9.64	76.75	12.57	135.60	22.21
5	58.28	9.54	80.80	13.23	139.08	22.78
6	58.24	9.53	82.33	13.48	140.57	23.02
DEM Resolution 10 m						
Number of Gauges	Over Estimate km^2	Over Estimate %	Under Estimate km^2	Under Estimate %	Total Disagreement km^2	Error Percentage %
2	53.21	8.72	126.63	20.74	179.84	29.45
3	58.61	9.59	76.19	12.47	134.81	22.08
4	58.64	9.60	74.08	12.13	132.71	21.73
5	58.07	9.51	78.02	12.77	136.09	22.29
6	58.06	9.50	79.44	13.01	137.51	22.52
DEM Resolution 1 m						
Number of Gauges	Over Estimate km^2	Over Estimate Percentage	Under Estimate km^2	Under Estimate Percentage	Total Disagreement km^2	Error Percentage
2	53.32	8.73	126.65	20.74	179.98	29.47
3	58.73	9.61	76.24	12.49	134.99	22.11
4	58.75	9.62	74.13	12.14	132.89	21.76
5	58.20	9.53	78.04	12.78	136.24	22.31
6	58.19	9.53	79.46	13.01	137.66	22.54

Underestimation Or Overestimation?

It is noteworthy that for flood mitigation and planning purposes, it is better to overestimate rather than underestimate; it is better to be too prepared than being unprepared (thus increasing vulnerability). Based on this argument, the four (4) stream gauges scenarios have the highest overestimation and the lowest underestimation consistently among the different DEM comparisons. This may be connected to the locations and/or the distances between those stream gauges in the combination of stream gauges used in that scenario. Figure 26-a shows the differences for the used DEM resolutions in km^2, while Figure 26-b shows those differences in error in a percentages format.

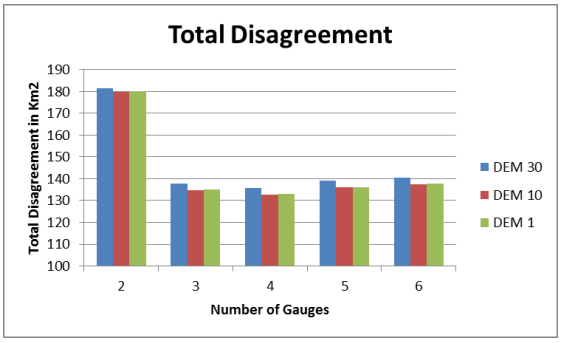

Figure 26-a

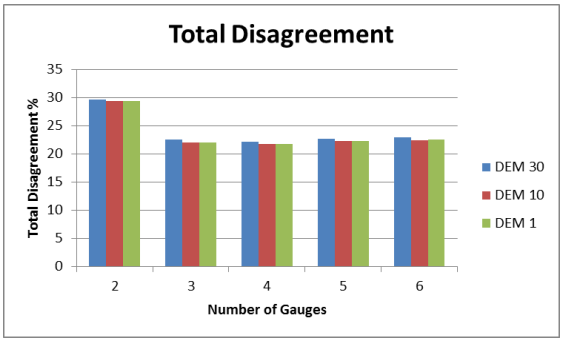

Figure 26-b

Figure 26: Comparison of results from various simulations in a bar style chart.

The results indicate that the two (2) stream gauges scenarios have the highest total error across all three different DEM resolutions. Thus, the same charts were created again, but without the two stream gauges cases to better show the comparison between the remaining of the simulated cases. Figures 27-a and 27-b show the differences for the used DEM resolutions without the two (2) stream gauges scenario. Similarly, Figures 28-

a and 28-b uses scatter graphs to show those differences for the used DEM resolutions simulations, again without including the two stream gauges case.

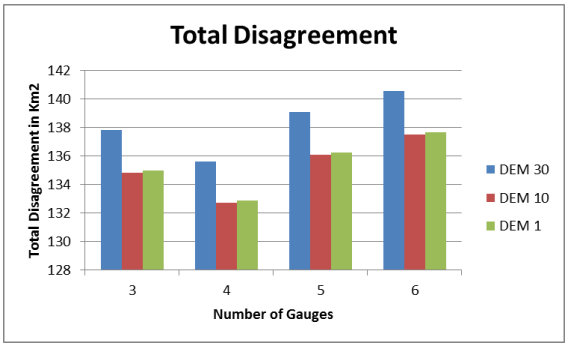

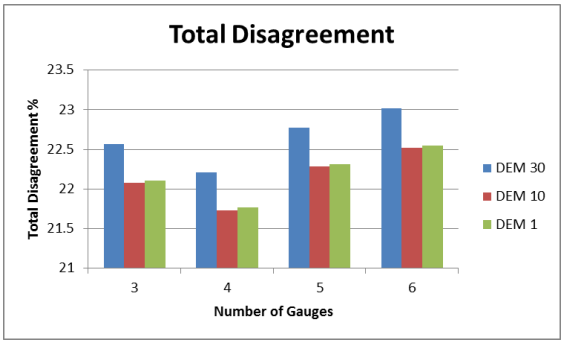

Figure 27-a Figure 27-b

Figure 27: Comparison of results from various simulations in a bar style chart, without the two stream gauges scenario.

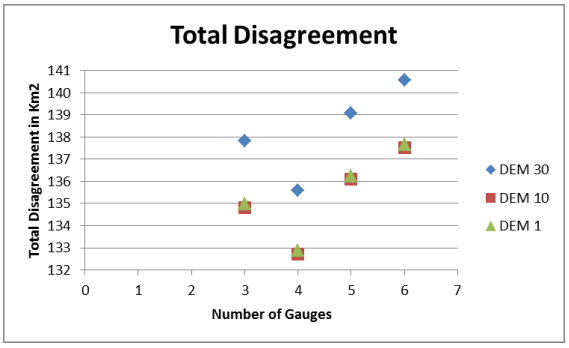

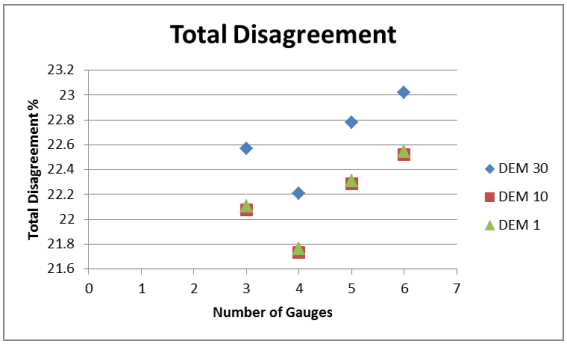

Figure 28-a Figure 28-b

Figure 28: Comparison of results from various simulations in a scatter style chart, without the two stream gauges scenario.

The charts above show more clearly that there is a higher difference between the 30m DEM and 10m resolutions, than there is between the 10m and 1m resolutions. These charts support the hypothesis that the higher the DEM resolution is, the lower the error will be. To further validate this claim, and to further compare the results, the same charts were created, again, without the scenario using two (2) stream gauges, as well as, without

the 30m DEM resolution. Figures 29-a and 29-b show the differences for the 10m and the 1m DEM resolutions without the two (2) stream gauges or the 30m DEM resolution scenarios. In the same fashion, Figure 30-a and 30-b uses scatter graphs to show those difference for the 10m and 1m DEM resolutions simulations, again without including the two (2) stream gauges nor the 30m DEM resolution cases.

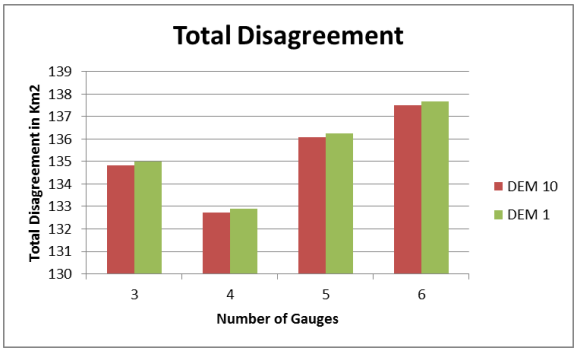

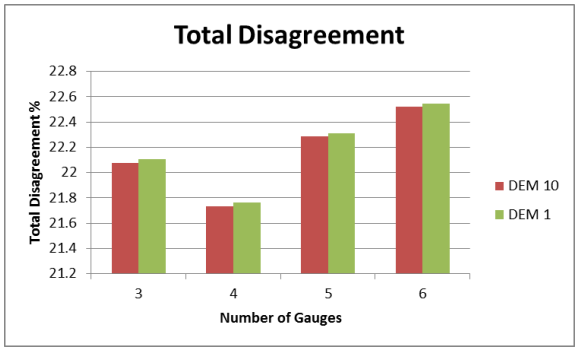

Figure 29-a Figure 29-b

Figure 29: Comparison of results from various simulations in a bar style chart, without the 30m DEM or the two stream gauges scenarios.

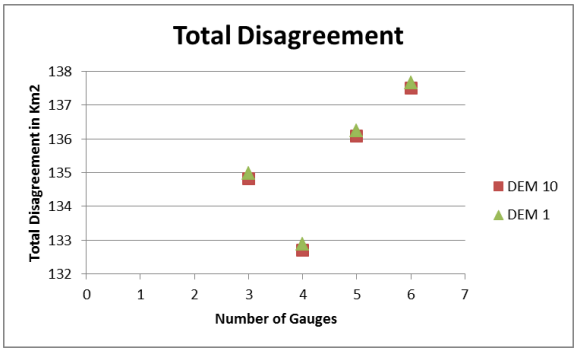

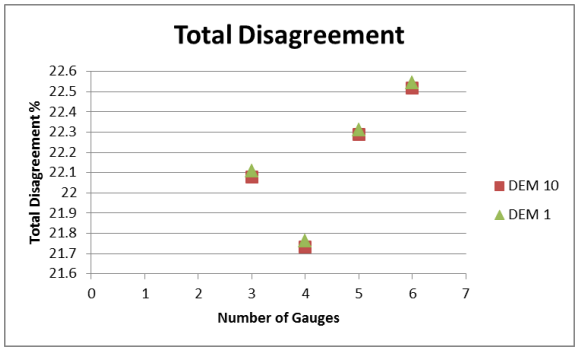

Figure 30-a Figure 30-b

Figure 30: Comparison of results from various simulations in a scatter style chart, without the 30m DEM or the two stream gauges scenarios.

The last set of charts shows that the difference in total disagreement is not significant between the 10m and 1m DEM resolution. In fact, it shows that the hypothesis is not totally true. In fact, surprisingly, these charts show slightly more total error in the 1m DEM compared to the 10m DEM resolution. Comparisons between single stream gauges scenarios were conducted between the 10m and 1m DEM resolution to compare the differences. The individual differences among the distribution scenarios were too small to have significance on the results. A quick statistical comparison between the results of these charts shows that the average difference in this point-to-point comparison between the 10m and 1m DEM resolutions in km^2 was 0.16 km^2, while in total percentage it was only 0.03%.

CHAPTER IV

DISCUSSION

Focus on Disagreement

It is important to realize that the model in this study simulated the flood based solely on elevation. As shown in Figure 31, some of the associated total disagreement may be, in fact, because of human influence on nature. Furthermore, Figure 32 shows that even during base flow conditions the stage of the river would be higher than the land elevation. Thus, the area would always be simulated as being flooded. In the Figure, the green areas that represents over estimations are actually agricultural fields protected by a levee. However, since those fields have low elevations, the model simulated them to be flooded. Similarly, in the same area of Peoria County mentioned with the over-estimation error, the area shaded in red is a reservoir. Since the reservoir borders are of high elevation, the model simulated that the water will not flood into the reservoir. It is noteworthy to mention that the error is controlled by human influences, which modify, mask or alter the real situation. To better show the differences elevation in the two mentioned cases, two elevation profiles were created. The first profile is for the agricultural fields and is represented by the A-A' line in Figure 31 (Figure 32). The second profile is for the reservoir and is represented by the B-B' line (Figure 33).

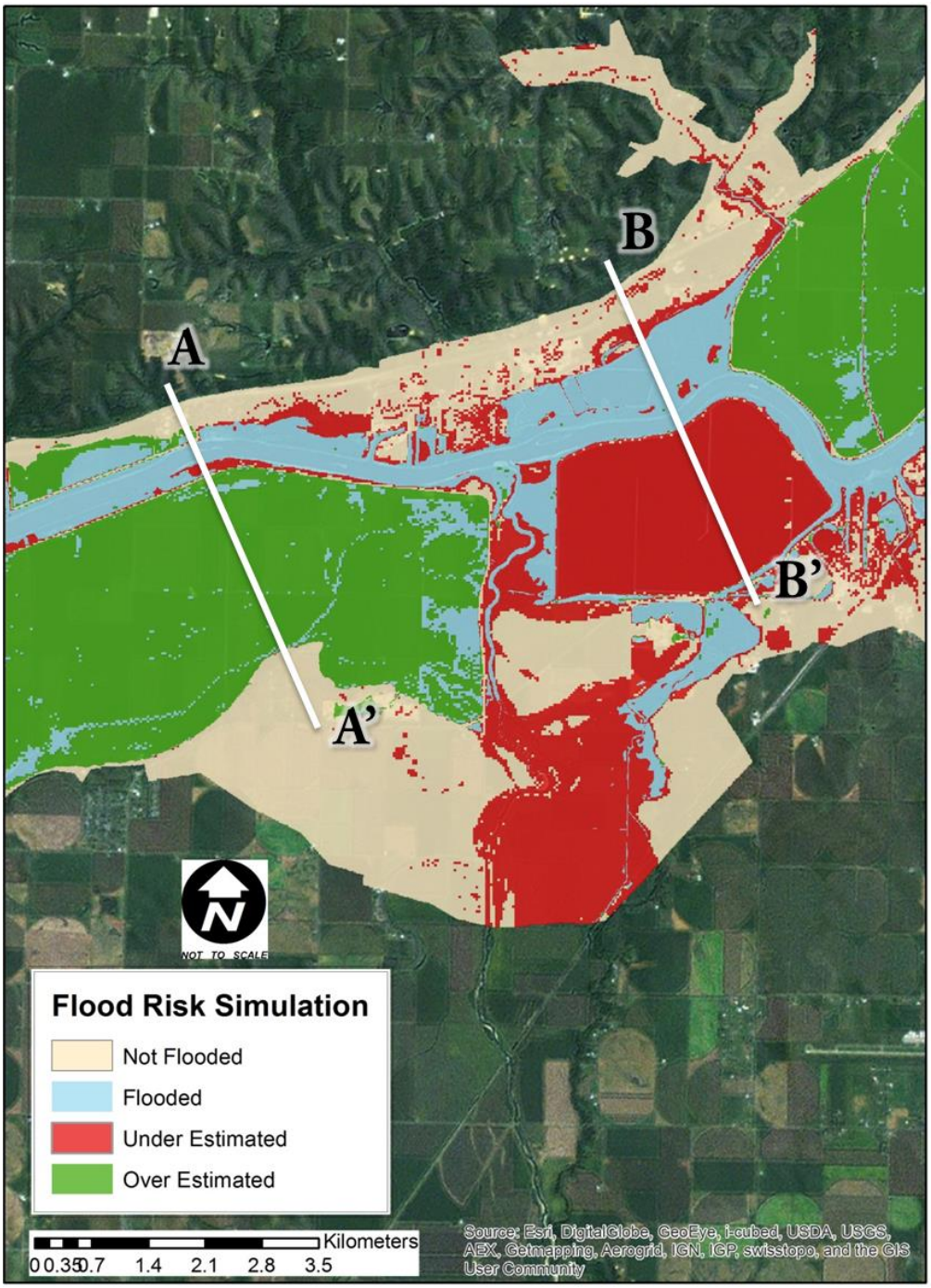

Figure 31: Map showing an example of the total disagreement associated with human modification of nature. Lines A-A' and B-B' show the location of the elevation profiles used for the agricultural fields and the reservoir, respectively

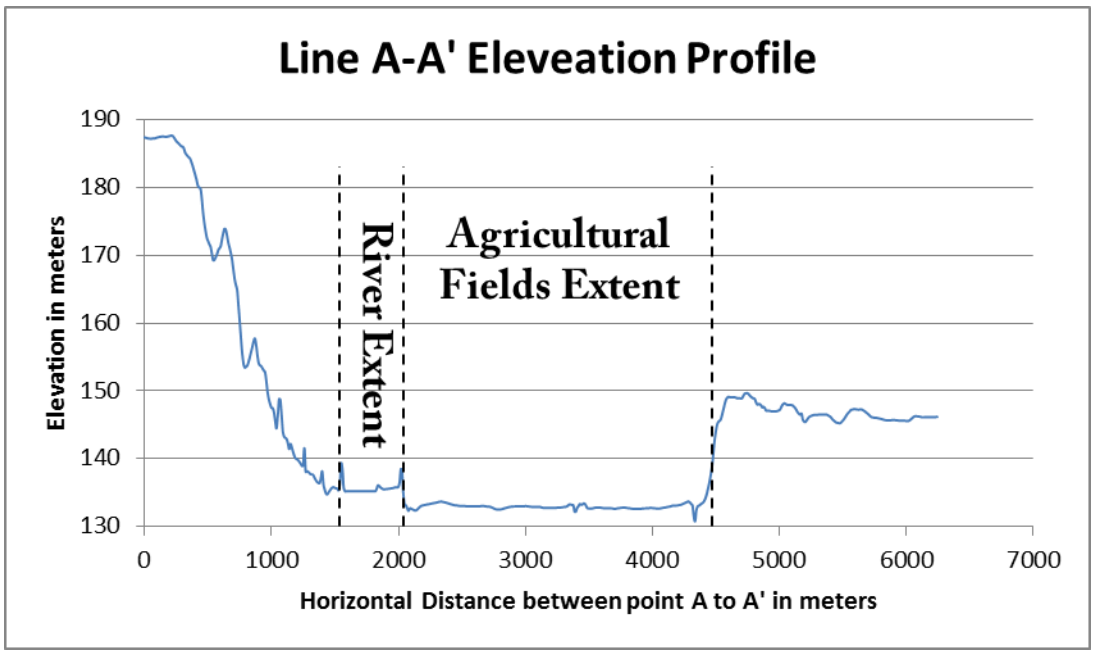

Figure 32: Line A-A’ elevation profile with the extent of river and agricultural fields

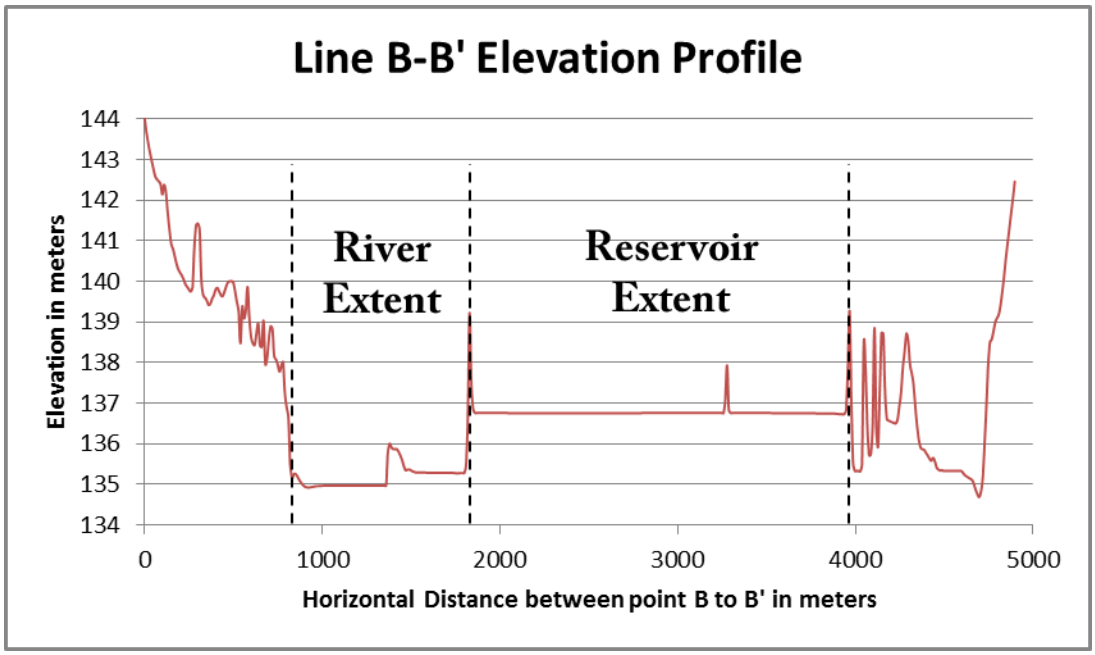

Figure 33: Line B-B’ elevation profile with the extent of river and the reservoir

It should be noted that in order to validate these methods Landsat imagery was acquired to represent the actual water on the day of the flood that hit the City of Peoria on April 23, 2013. However, since that day was the day of peak flooding, it means that it was also a day of heavy rain and/or severe weather conditions, the Landsat imagery for April 23rd was covered with clouds and unusable. Thus, a later date was chosen that had Landsat imagery with less atmospheric interference. As the hydrograph (Figure 34) shows, April 29th is after the peek but is still considered a point of high flood stage. This could justify some of the underestimation in the simulation. In other words, the areas at which the model predicted an area as not flooded but were actually flooded may be a result of residual flooding associated with the peak conditions. Regrettably, there is no way to validate that without having a Landsat imagery that corresponds to the day of the flood, which is, quite frankly, not likely most of the time.

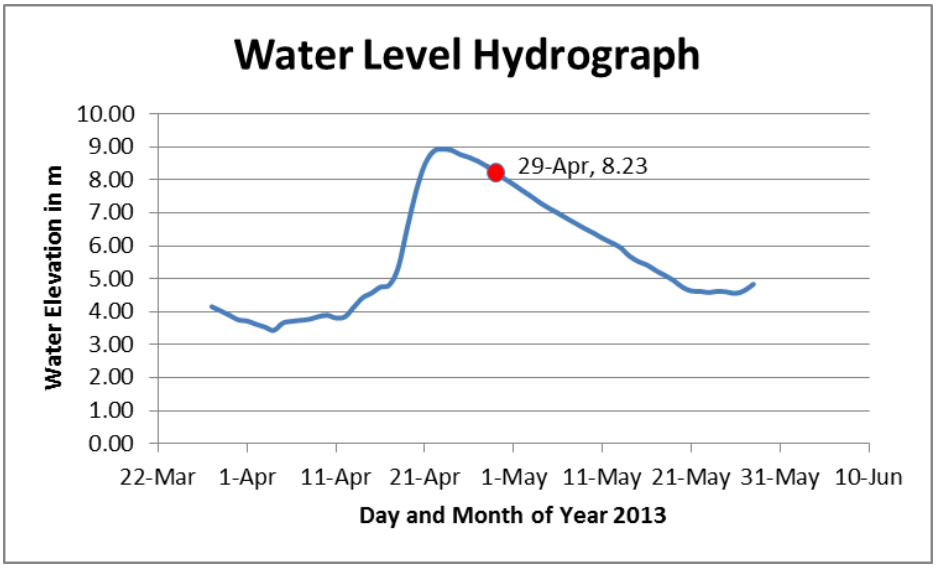

Figure 34: Hydrograph of gauge Peoria (prai2) showing the peak, and position of the Landsat imagery date

Total underestimation should also be examined more specifically. Figure 35 shows only the under estimated areas in the four stream gauges case on a 10m DEM and suggests that one possible explanation for the high underestimation is because the land is still wet with residual water following the peak conditions. Furthermore, the elevation of the land (the primary factor in the flood model) suggests that it should be dry. During the rising limb of the hydrograph it may have been dry, but as the flood recedes the water may have stayed in small depressions, showing up in the classification of the Landsat data and skewing the resulting comparative analysis. This gives some explanation for why the error tends to be fairly consistent with the various DEM resolutions. Nevertheless, looking at the maps visually might give insight into why this is the case.

Another analysis of the error was a spatial analysis that aims to find out if the error in overestimation is always lower than under estimate, or if there is a point where they flip. Figures 36, 37, and 38 show comparisons between overestimate and under estimate for the different DEM resolutions used in the simulation. It is clear that the error seems constant and there is no flip point.

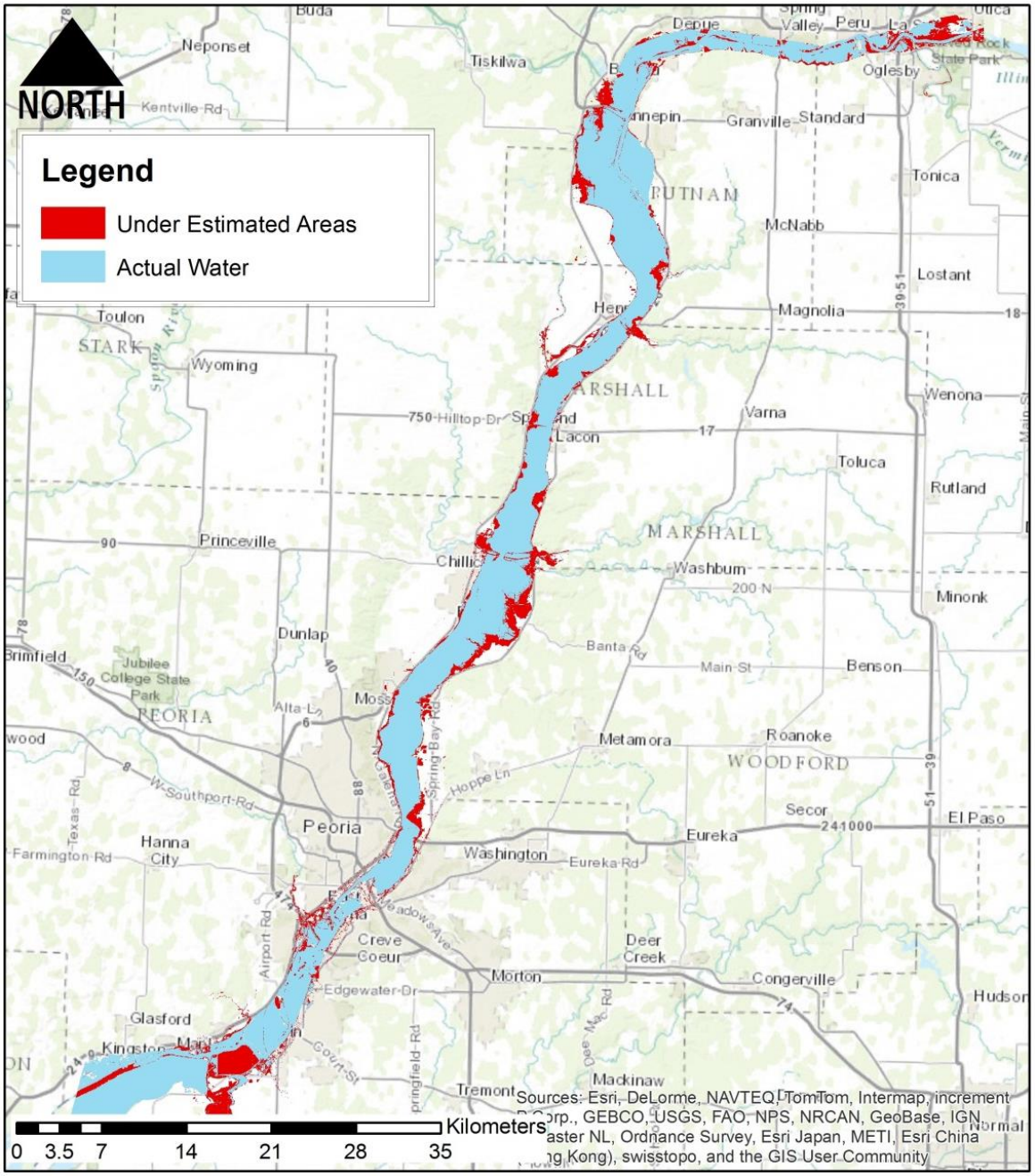

Figure 35: Underestimation map for the 4 stream gauges, 10m DEM Resolution

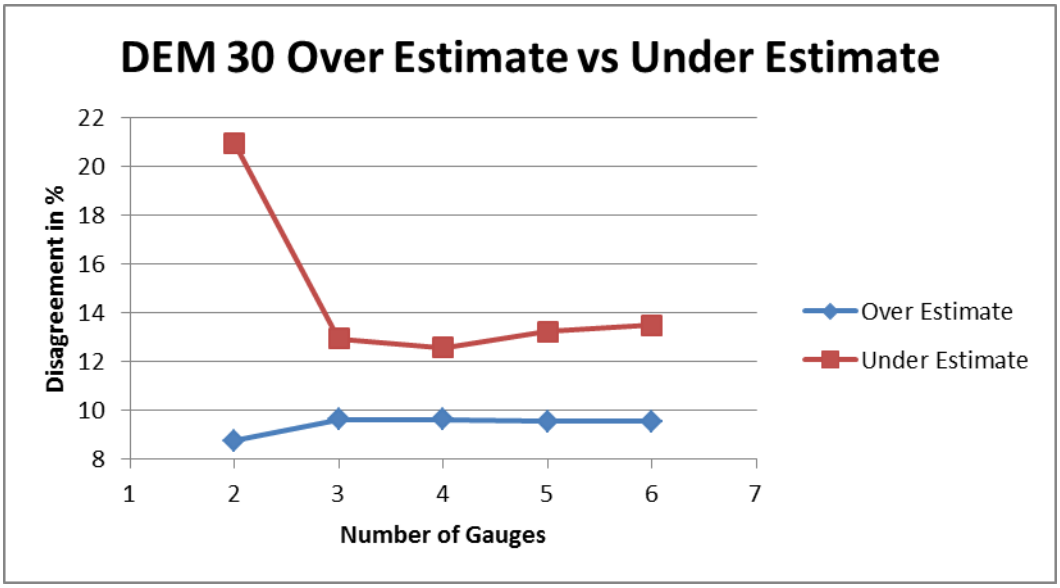

Figure 36: Overestimation vs. Underestimation comparison, 30m DEM resolution

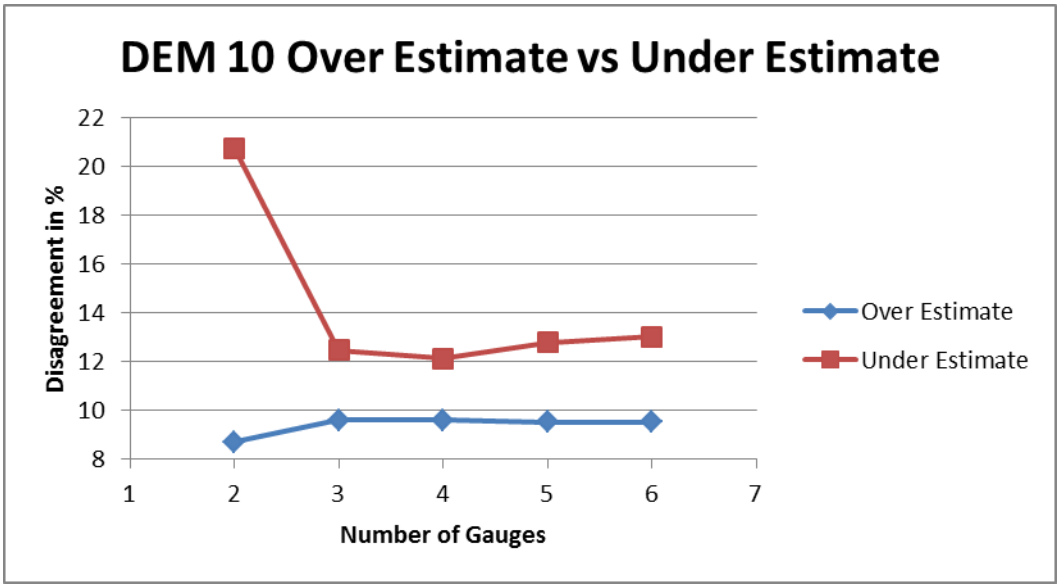

Figure 37: Overestimation vs. Underestimation comparison, 10m DEM resolution

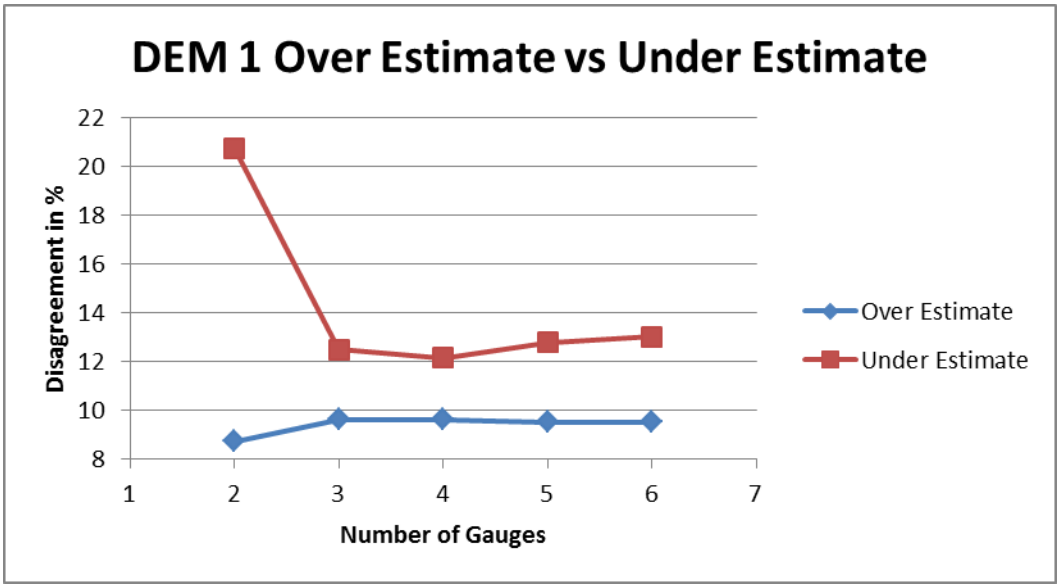

Figure 38: Overestimation vs. Underestimation comparison, 1m DEM resolution

Final disagreement analysis was done to compare all overestimations for the different DEM resolutions, as well as all underestimations, as a profile comparison. Figure 39 shows a comparison between the flood risk simulation overestimations for the different DEM resolutions.

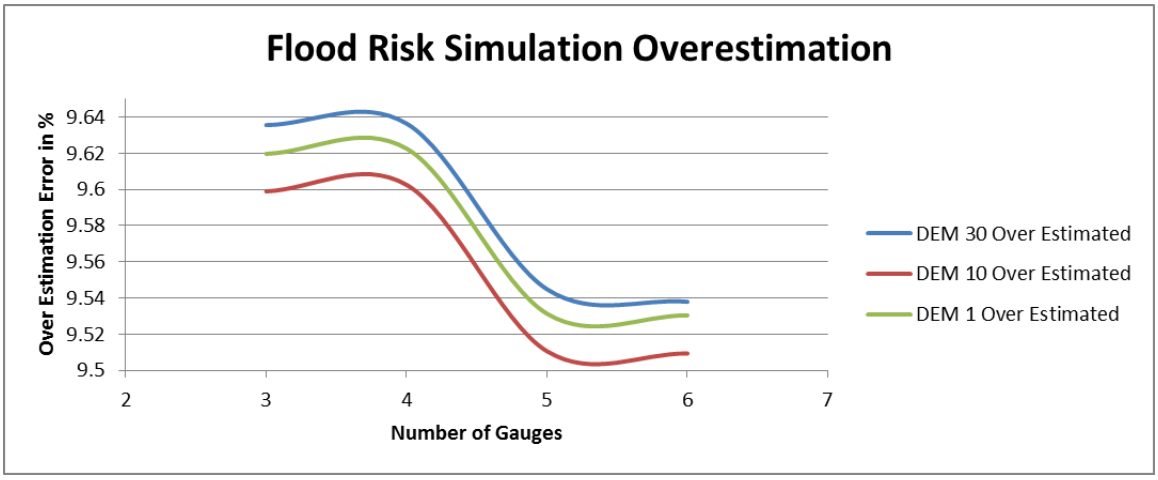

Figure 39: Flood Risk Simulation Overestimations

Likewise, Figure 40 shows a comparison between the flood risk simulations underestimations for the different DEM resolutions used in this study. Looking at Figure 40, only the 30m DEM has a clear higher error percentage.

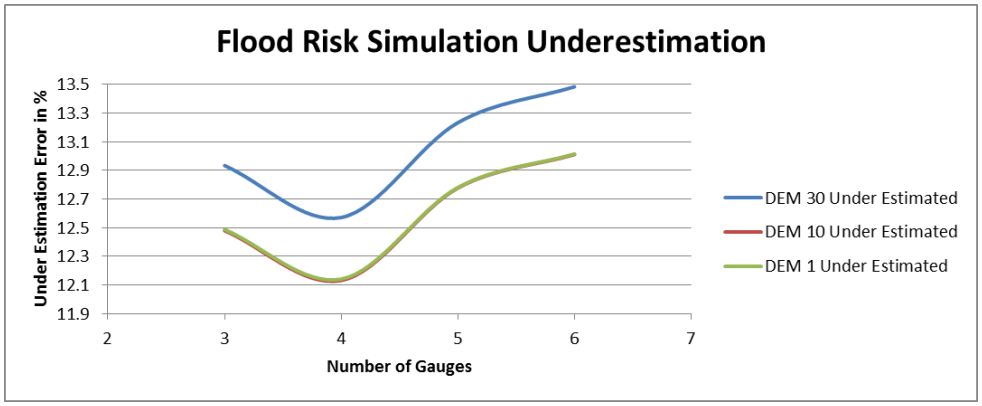

Figure 40: Flood Risk Simulation Underestimations

Although the two lines seems identical, there is only a slight improvement in reducing the error percentage between the 10m and the 1m DEM resolution when using the four (4) stream gauges scenario. However, as shown in Figure 40 above, this improvement is only 0.03%, according to the accuracy assessment.

CHAPTER V

CONCLUSIONS

The results in this study were somewhat different than what was anticipated. Only one of the hypotheses was supported with project results; specifically, it was found that it is possible to create flood prediction maps using few data inputs. The highest error percentage is less than 30%, and if the 2 stream gauges case scenario was excluded the highest error percentage in only 23%. It is noteworthy that even though the numbers may seem large, the study error percentages represent the least amount of data possible to create a decent flood risk analysis map, which include digital elevation models (DEM) and definable stream gauges water level in this case.

The second and third hypotheses, however, were found not to be completely true. For instance, the hypothesis that highly detailed data will result in better simulations and will give the results a better meaning was not justified by the results. Even though the simulations using the 30m DEM resolution have higher total disagreement compared to the 10m DEM resolution, the 1m DEM also, surprisingly, have a higher total disagreement. A logical explanation was found in a release note provided by the USGS regarding the National Elevation Dataset (NED). The NED metadata states that the study area extent is within the Missouri and Mississippi River Basin flood project for the Corp of Engineers for the Upper Midwest and Plains States, which lasted from 1997 to 2001

using 1/9 arc second (3m) National Elevation Dataset. Later on, the 3m LiDAR DEMs were used to create the 10m and the 1m DEM resolutions (USGS, 2002). This explains why the results between the two DEM resolutions were close; they are derived from the same elevation source. This suggests that the source elevation data is more important than the spatial resolution of the DEM. On the other hand, there are two different versions of standard 30m DEM modules in the United States: "Level 1" and "Level 2". The 30m DEM used in this study is a "Level 1" 30m DEM which was derived from 7.5 US Topo maps, also created by the USGS (USGS, 2002). While "Level 2" 30m DEMs are derived from 1/3 arc second DEMs, which are usually 10m DEMs (USGS, 2002). This different elevation source explains, in part, why the 30m DEM used in this study yielded different results than the other DEM resolutions, and that is because, being a "Level 1", it was derived from a very different elevation source than the 10m and 1m DEMs. It is, however, important to realize that, according to the results in table 2, the difference between the 10m DEM and the 1m DEM resolutions simulations is not significant, and the results should not directly give priority to, impact, or influence the choice of what DEM resolution for use in simulating a flood with similar characteristics to the study area of this study. As a matter of fact, despite the fact that the 30m DEM resolution is not as good as the LiDAR derived 10m and 1m DEMs, the differences are surprisingly small. Considering the cost of acquiring a LiDAR, as well as the longer processing times (Figure 41), the results from this study suggests that the 10m DEM resolution should be an adequate substitute for both the 30m and the 1m DEM resolutions, since it has better results than the 30m DEM and about 1/3 the processing time of the 1m DEM. Equally

important, the fact that the 1m and the 10m results are very similar, suggests that the spatial resolution is not a big influence IF the source elevation data (LiDAR) is the same for both DEMs, as it is the case in the study in hand, or for an area with similar characteristics of the study area.

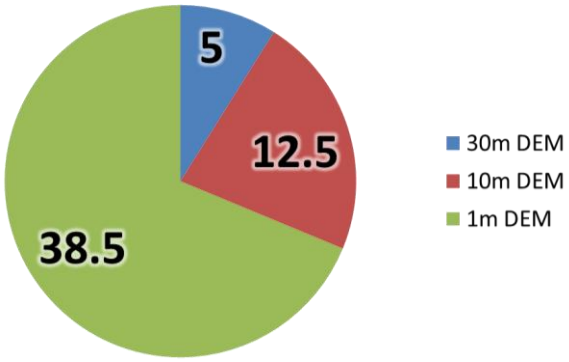

Figure 41: Comparison of analysis time in minutes for the different DEM resolutions

The third and final hypothesis that focused on the number of stream gauges was also largely unsupportable. Surprisingly, the four (4) stream gauges scenario has the highest over estimate and the lowest under estimate across all three resolutions, as well as, the least error percentage. It seems that, again, the middle density has the best results. Regardless of the DEM resolution used, the four (4) stream gauge distribution has the best results based on the previously mentioned argument to focus on disagreement as underestimation and overestimation. One or a combination of factors may have led to these results. It is possible that the four-gauge scenario, illustrated in Figure 8, has an optimal spatial distance and/or distribution of the gauges. Another possibility is that it may have taken out some of the gauges that have higher error. One more possibility is that the interpolation method used, the IDW, in the study area's settings has a threshold

that was reached with four (4) gauges, and the results just do not get better with more gauges. A future study may try the different distributions and combinations than those used in the current study. This would evaluate if it is connected to the location and distance, or it may find a different interpretation.

Future Use of the Model

The simplicity of this model makes it a great asset in urban planning and future flood predictions. For instance, if an area is expecting a flood of a certain intensity, all they need to do is to use a DEM and a stream gauge, both data can be acquired for free, and plug them into the model. In addition, if an organization has its own data, the same methodology can be used for on the fly flood vulnerability predications. This would help decision makers to predict, quickly, a coming flood. Furthermore, this simplified model is easier to implement by a wide range of staff and personnel, especially those who are not flood engineers. In addition, this simulation should be applicable worldwide with any DEM resolution or gauges density. This was proved since the topo maps derived 30m DEM resolution yielded results that are similar to the LiDAR derived 10m and 1m resolutions.

REFERENCES

Al-Sabhan, W., Mulligan, M., Blackburn, G., 2003. A real-time hydrological model for flood prediction using GIS and the WWW. Computers, Environment and Urban Systems, v.27, no. 1, p. 9-32, doi:10.1016/S0198-9715(01)00010-2.

Arnell, N.W., Reynard, N.S., 1996. The effects of climate change due to global warming on river flows in Great Britain: Journal of Hydrology., v. 183, no. 3-4, p. 397-424, doi:10/1016/0022-1694(95)02950-8.

Barroca, B., Bernardara, P., Mouchel, J., Hubert, G., 2006. Indicators for identification of urban flooding vulnerability. Natural Hazards and Earth System Sciences, 6, 553-561.

Beffa C., 1998. Two-Dimensional Modelling of Flood Hazards in Urban Areas. Proc. 3rd Int. Conf. on Hydroscience and Engineering, D-Cottbus., or http://www.fluvial.ch/pub.html

Beffa, C., 2000. A Statistical Approach for Spatial Analysis of Flood Prone Areas, International Symposium on Flood Defence, September 20-23, 2000, D-Kassel

Cameron, D. S., Beven, K., J., Tawn, J., Blazkova, S. and Naden, P., 1999. Folld frequency estimation for a gauged upland catchment (with uncertainity), Journal of Hydrology. V.219, no. 3-4, p. 168-187. doi: 10.1016/S0022-1694(99)00057-8

City of Peoria website, http://www.peoriagov.org/mayors-office/april-2013-flood/

Connell R. J., Beffa C., and Painter D. J., 1998. Comparison of observations by flood plain residents with results from a two-dimensional flood plain model. J. of Hydrology. New Zealand, p 55-79.

El-Hames, A.S. and Al-Wagdany, A.S., 2012. Reconstruction of flood characteristics in urbanized arid regions: case study of the flood of 25 November 2009 in Jeddah, Saudi Arabia. Hydrological Sciences Journal, v.57 no.3, p. 507-516. doi: 10.1080/02626667.2012.665995

El-Hames, A.S. and Richards, K.S. 1998. An integrated, physically based model for arid region flash flood prediction capable of simulating dynamic transmission loss. Hydrological Processes, v. 12, no.8, p. 1219–1232. doi: 10.1002/(SICI)1099-1085(19980630)12:8<1219::AID-HYP613>3.0.CO;2-Q

Environmental Systems Research Institute, Inc. (Esri): http://www.esri.com/

Farmahan, Inderpreet Singh, GIS is a Powerful Tool for Local Governments (February 7, 2012). City and Town, Arkansas Municipal League, February 2012.

Hansson, K., Danielson, M., Ekenberg, L., 2008, Assessment of a flood management framework, International Journal of Public Information Systems, v.4, no.1, p.25-37

Hulme, M., Barrow, E.M., Arnell, N.W., Harrison, P.,A., Johns, T.C, and Downing, T.E. 1999. Relative impact of human-induced climate change and natural climate variability, Nature, v. 397, p 689-691, doi: 10.1038/17789

Illinois State Geological Survey: http://www.isgs.uiuc.edu/nsdihome/webdocs/ilhmp/

Kia, M., Pirasteh, S., Pradhan, B., Mahmud, A., Sulaiman, W., Moradi, A., 2012, An artificial neural network model for flood simulation using GIS: Johor River Basin, Malaysia, Environmental Earth Science, v.67, p. 251-264, doi: 10.1007/s12665-011-1504-z

Lawrence, J., Xelrod, A., Timothy, M., Perceptions of ecological risk from natural hazards, Decision Research, Journal of Risk Research, v.2, no.1, p.31-53, doi: 10.1080/136698799376970

Lian, Y., Chan, I., Xie, H., and Demissie, M., 2010, Improving HSPF Modeling Accuracy from FTABLES: Case Study for the Illinois River Basin, Journal of Hydrologic Engineering, v.15, no. 8, p. 642-650, doi: 10.1061/(ASCE)HE.1943-5584.0000222

McKee, F., 2002. The Importance of GIS in Modern Society and the Effective Partnering of Education and Industry, 5th AGILE Conference on Geographic Information Science, Palma (Mallorca, Spain) April 25th-26th 2002.

Naden, P., Crooks, S., Broadhurst, P., 1998, Impact of climate and land use change on the flood response of large catchments, Proc. 31st MAFF Conference of River and Coastal Engineers, Keele, UK, July 1996, 2.1.1-2.1.16

National Association of Counties: http://www.naco.org

National Elevation Data Set, USGS, 2002: http://ned.usgs.gov/

National Hydrography Dataset: http://viewer.nationalmap.gov/viewer/nhd.html?p=nhd

NOAA National Weather Service: http://www.weather.gov

Norheim, R.A., Queija, V.R., Haugerud, R.A., 2002. Comparison of LiDAR and INSAR DEMs with dense ground control, in proceedings, 2002 ESRI International User Conference, San Diego, California, 8-12 July 2002: paper 0442.

Panagoulia, D., Dimou, G., 1997. Sensitivity of flood events to global climate change, Journal of Hydrology, v. 191, no. 1-4, p. 208-222, doi: 10.1016/S0022-1694(96)03056-9

Piling, C., Wilby, R., Jones, J., 1998. Downscaling of catchment hydrometeorology from GCM output using airflow in upland wales, Hydrology in a Changing Environment: Proceedings of the British Hydrological Society International Conference, Exeter, July 1998, v.1, p. 191-208

Polechla, P.J., Carrillo-Rubio, E. and Suzan, G. et al., 2006, First wildlife law in the borderlands of Mexico and U.S.A.: beavers and river otters. Book chapter. In: P.J. Polechla. The river otters of the southwestern U.S. and Mexico: past, present, and future. Cincar Publishing, Socorro, NM.

Price, M., 2012, Mastering ArcGIS Fifth Edition: New York, McGraw-Hill, 612, ISBN-10: 0077462955

Safaripour, M., Monavari, M., Zare, M., Abedi, Z., Gharagozlou, A., 2012, Flood Risk Assessment Using GIS (Case Study: Golestan Province, Iran) ,Polish Journal of Environmental Studies, v. 21, no. 6, p. 1817-1824, ISSN: 1230-1485

Sinnakudan, S., Ghani, A., Ahmad, M., Zakaria, N., 2003, Flood risk mapping for Pari River incorporating sediment transport, Environmental Modelling & Software, v. 18, no. 2, p. 119-130, doi: 10.1016/S1364-8152(02)00068-3

Smemoe, Christopher M., E. James Nelson, Alan K. Zundel, and A. Woodruff Miller, 2007. Demonstrating Floodplain Uncertainty Using Flood Probability Maps. Journal of the American Water Resources Association, v. 43, no. 2, p. 359-371, doi: 10.1111/j.1752-1688.2007.00028.x

United States Army Corps of Engineers (USACE), 2004, "Upper Mississippi River system flow frequency study." Final Rep., USACE Rock Island District, Ill.

USGS Global Visualization Viewer: http://glovis.usgs.gov/

Watson, D. F., and G. M. Philip, 1985. A Refinement of Inverse Distance Weighted Interpolation. Geoprocessing v.2, p.315–327, ISSN: 0165-2273

Wigley, T., Raper, S., 1992. Implications for climate and sea level of revised IPCC emission scenarios, Nature, v. 357, p. 293-300, doi:10.1038/357293a0

Worthen, A. W., 1868, Geology of Illinois, the Legislature of Illinois, ISSN-10: 124819909X

Yalcin, G., Akyurek, Z., 2004, Analyzing flood vulnerable areas with multicriteria evaluation, XXth International Society for Photogrammetry and Remote Sensing Congress.